

# LIVARSKI VESTNIK

61/2014

3



DRUŠTVO LIVARJEV SLOVENIJE  
SLOVENIAN FOUNDRY MEN SOCIETY

*swatyComet*



SPARKS WORLD

SWATYCOMET

umetni örusi in nekovine; d.o.o.

Tirova cesta 60, 2000 Maribor, Slovenijo, EU

T: +386 (0)2 333 16 00 - F:+386 (0)2 333 17 90

E-mail: [info@swatycomet.si](mailto:info@swatycomet.si)



[www.swatycomet.si](http://www.swatycomet.si)



# TERMIT

## PROIZVODNI PROGRAM:

- KREMENOV PESEK
- KERAMIČNI PESEK
- OPLAŠČENI KREMENOMI  
IN KERAMIČNI PESKI
- OGNJEVZDRŽNI PREMAZI
- POMOŽNA LIVARSKA SREDSTVA



# EXOTERM-IT

MATERIALS FOR MELTING SHOP-  
RECARBURISER, INOCULANTS  
AND FERROALLOYS

COATINGS AND ADDITIVES  
FOR SAND CORES  
AND FOR SAND MOULDS

EXOTHERMIC MATERIALS, FEEDER  
SLEEVES AND OTHER AUXILIARIES

EXOTHERMIC AND INSULATING  
MATERIALS FOR STEEL WORKS

CASTING TECHNOLOGY WITH

**MAGMA**

# FerroECOBlast® EUROPE

Since 1964

SOLUTIONS FOR FOUNDRY INDUSTRY

[www.ferroECOBlast.com](http://www.ferroECOBlast.com)

Do you have complicated diverse casting molds which demand **100 % cleanliness**?



Complex diverse castings where it's difficult to clean all angles at 100 %

Cleaning very thin products is our specialty



Rotating step by step

Big complex castings which can't fit into your ordinary wheel blast machine

#### WE GUARANTEE YOU

- latest technology solutions
- reliable & non-stop production
- best efficiency / energy ratio
- short run delivery terms
- aftersales response in 24 hours
- work-safe and environmental-friendly



What can FerroECOBlast® do for you:

- Controlled cleaning process, especially inside and on the close corners
- Full automation of the whole blasting process
- Suggest latest and best solution for your problem



Small and diverse series - manual or half automated work

## Custom made solutions



Inspected for 100 % cleanliness



Deburring of aluminium alloys castings



Automatic and controlled blasting process



Complex blasting solutions and full automatization

FerroCrtalic d.o.o., tel +386 (0)7 38 45 100 & fax +386 (0)7 38 45 115,  
[info@ferrocrtalic.com](mailto:info@ferrocrtalic.com) / [www.ferroECOBlast.com](http://www.ferroECOBlast.com)

# LIVARSKI VESTNIK

**Izdajatelj / Publisher:**

Društvo livarjev Slovenije  
Lepi pot 6, P.P. 424, SI-1001 Ljubljana  
Tel.: ++ 386 1 25 22 488  
Fax: ++386 1 426 99 34  
E-mail: [drustvo.livarjev@siol.net](mailto:drustvo.livarjev@siol.net)  
[www.drustvo-livarjev.si](http://www.drustvo-livarjev.si)

**Glavni in odgovorni urednik /****Chief and responsible editor:**

prof. dr. Alojz Križman  
E-mail: [probatus@triera.net](mailto:probatus@triera.net)

**Tehnično urejanje / Technical editing:**

mag. Mirjam Jan-Blažič

**Uredniški odbor / Editorial board:**

prof. dr. Alojz Križman, Univerza v Mariboru  
prof. dr. Primož Mrvar, Univerza v Ljubljani  
prof. dr. Jožef Medved, Univerza v Ljubljani  
doc. dr. Gorazd Lojen, Univerza v Mariboru  
prof. dr. Andreas Bührlig-Polaczek, Giesserei  
Institut RWTH Aachen  
prof. dr. Peter Schumacher, Montanuniversität  
Leoben  
prof. dr. Reinhard Döpp, TU Clausthal  
prof. dr. Jozef Suchý, AGH Krakov  
prof. dr. Jaromír Roučka, Institut Brno  
prof. dr. Faruk Unkić, Univerza Zagreb  
dr. Milan Lampič, Fritz Winter, Stadtallendorf

**Prevod v angleški jezik /****Translation into English:**

prof. dr. Andrej Paulin, Darja Srakar-Tomanič

**Lektorji / Lectors:**

Angleški jezik / English:  
dipl. ing. Peter Haensel, Düsseldorf  
Slovenski jezik / Slovene:  
prof. Janina Šifrer

**Tisk / Print:**

Fleks d.o.o.

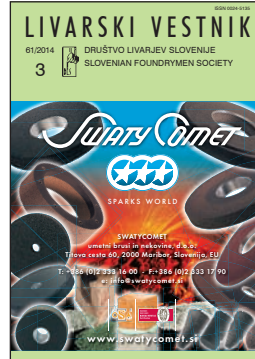
**Naklada / Circulation:**

4 številke na leto / issues per year  
800 izvodov / copies

**Letna naročnina:** 35 EUR z DDV

**Year subscription:** 35 EUR (included PP)

Dano v tisk: september 2014



**Naslov/Adresss:**  
SWATYCOMET, umetni brusi  
in nekovine, d.o.o.  
Titova cesta 60  
2000 Maribor  
Slovenia

**Direktor:** Matjaž Merkan

T: +386 (0)2 333 16 00  
F: +386 (0)2 333 17 90  
W : [www.swatycosmet.si](http://www.swatycosmet.si)  
E : [info@swatycosmet.si](mailto:info@swatycosmet.si)

## VSEBINA / CONTENTS

Stran / Page:

Janko Ferčec, Rebeka Rudolf: Nikelij-titanova zlitina za ortodontsko žico za loke: izdelava, funkcionalne lastnosti in biokompatibilnost / Nickel-titanium alloy for orthodontic arch-wire: Manufacture, functional properties and biocompatibility

61

S. Müller, H. Pries, K. Dilger: Izboljšanje procesa načrtovanja hladilnih sistemov pri kokilah za tlačno litje - občuten prispevek h kakovosti in življenjski dobi / Enhancing the Design Process of Cooling Systems for Die-Casting Dies - A Significant Contribution to Quality and Lifetime

134

György Fegyvernek, Monika Tokár: Preiskava trdnostnih lastnosti ulitkov za avtomobilsko industrijo, izdelanih iz livnih Al-Si zlitin / The examination of the strength properties on the vehicle industry castings produced from Al-Si foundry alloys

153

## AKTUALNO / ACTUAL

- |  |     |
|--|-----|
| Euroguss 2014 v Nuernbergu   | 161 |
| 71. WFC- svetovni lивarski kongres   | 162 |
| In memoriam: Jakob Mostar  | 163 |
| 55. mednarodno liversko posvetovanje Portorož 2015/<br>55 <sup>th</sup> International Foundry Conference Portorož 2015 | 164 |

Izdajanje Livarskega vestnika sofinancira Javna agencija za raziskovalno dejavnost Republike Slovenije  
Publishing supported by Slovenian Research Agency

Livarski vestnik je vpisan v razvid medijev Ministrstva za kulturo pod zaporedno številko 588

Janko Ferčec<sup>1</sup>, Rebeka Rudolf<sup>1,2</sup>

<sup>1</sup>Fakulteta za strojništvo, Univerza Maribor / Faculty of Mechanical Engineering, University of Maribor,  
Smetanova 17, 2000 Maribor, Slovenija / Slovenia

<sup>2</sup>Zlatarna Celje d.d., Kersnikova 19, 3000 Celje, Slovenija / Slovenia

## Nikelj-titanova zlitina za ortodontsko žico za loke: izdelava, funkcionalne lastnosti in biokompatibilnost

## Nickel–titanium alloy for orthodontic arch-wire: Manufacture, functional properties and biocompatibility

### Izvleček

Nikelj-titanove zlitine so postale zelo uporabljan material v medicinskih aplikacijah, še posebej za fiksne ortodontske aparate pri zdravljenju neporavnanih zob. Razlog je v tem, da imajo ti materiali funkcionalne lastnosti in da so biokompatibilni. Ta prispevek se osredotoča na pojasnitev procesa izdelave zlitin z oblikovnim spominom, na ugotavljanje njihovih funkcionalnih lastnosti ter na ugotovitev stopnje biokompatibilnosti. Pri ugotavljanju funkcionalnih lastnosti smo merili temperaturo faze, pri kateri ima zlitina z oblikovnim spominom popolno avstenitno mikrostrukturo. Nato smo ugotavljali mehanske lastnosti z enosnim nateznim preskusom. V delu biokompatibilnosti smo prikazali postopek, s katerim je mogoče oceniti biološko ustrezost ortodontskih žic.

Vsi ti rezultati nam posredno pomagajo pojasniti postopek in potek ortodontskega zdravljenja, še posebej za primer uporabe različnih komercialno dostopnih Ni-Ti ortodontskih žic.

**Ključne besede:** zlitine z oblikovnim spominom, izdelava, funkcionalne lastnosti, biokompatibilnost

### Abstract

Nickel-titanium alloys have become a widely used material in medical applications, especially in orthodontic appliances for treatment of protruding teeth. The reason for this is that this material has specific functional properties and is biocompatible. This paper concentrates on the clarification of the process of manufacture of shape memory alloys and determination of the functional properties and biocompatibility of different orthodontic wires from this alloy. When establishing the functional features, we first determined the temperature of the phase in which the shape memory alloy has completely austenitic microstructure. Then we determined the mechanical properties with a uni-axial tension test.

This helps in the understanding of orthodontic treatment using different commercially available orthodontic arch-wires from nickel-titanium alloy. In the section on biocompatibility the process of determining the biocompatibility of orthodontic wires is shown.

**Key words:** shape memory alloy, manufacture, functional properties, biocompatibility

## 1 Uvod

Žica iz zlitine z oblikovnim spominom se uporablja za številne pripomočke v medicini, vključno z vodilnimi žicami, katetri, žilnimi opornicami (stenti), filtri, iglami, vodilnimi čepi, endodontskimi pilami in ortodontski pripomočki. Pri ortodontski popravi naprej štrlečih zob se uporablja tehnika nežnega in stalnega pritiska na zobe. Sila, ki deluje na zob, ustvarja napetosti, ki delujejo najprej na zob, potem pa se te prenašajo na periodontalni ligament. Te napetosti nato povzročijo spremembe v prekrvavitvi periodontalnega ligamenta, kar vodi v preoblikovanje čeljusti. Istočasno se uporablja za pomik zoba v pravilno lego v ustni votlini. Za učinkovito delovanje sil na več zob hkrati se uporablajo fiksni ortodontski pripomočki (slika 1). Ti ortodontski pripomočki so sestavljeni iz konzol, ki so pritrjene na kruno zuba tako, da so prilepljene ali pritrjene na zob s posebnimi trakovi. Ko ortodont namesti konzole na vsak zob zgornje ali spodnje čeljusti, se uporabi ortodontska žica. Žica za loke, ki se vstavi v utore na konzolah, deluje s silo na zob, s čemer počasi pomika zob med zdravljenjem [1-3].



**Slika 1.** Ortodontski pripomoček iz nikelj-titanove ortodontske žice z oblikovnim spominom

**Figure 1.** Orthodontic appliance by SMA NiTi orthodontic wire

## 1 Introduction

Shape Memory Alloy (SMA) wire is used in a variety of medical device applications including guide wires, catheters, stents, filters, needles, guide pins, endodontic files and orthodontic appliances. In the process of the orthodontic treatment of protruding teeth the technique of a gentle and continuous force is used on the teeth. The force exerted on the tooth to create stresses acts first on the tooth and then it is transferred to the periodontal ligament. These stresses subsequently cause a change in the blood supply to the periodontal ligament, leading to the transformation of the jaw. At the same time, it is used to move teeth into their correct position in the oral cavity. For efficient operation of forces on several teeth at the same time fixed orthodontic appliances are used (Figure 1). These orthodontic appliances consist of brackets which are attached to the crown of the tooth so that they are glued or fastened to the teeth with special bands. When the orthodontist has placed the bracket on each tooth on the upper or lower jaw, the orthodontic wire is then introduced. The arch-wire, which is inserted into the slots in the brackets, causes force on the tooth and, consequently, the movement during the course of treatment [1-3].

The desirable properties of orthodontic wires are, mainly, the following: Good biocompatibility, good spring-back, good range, and tough and low friction. It's important also that the formability is resilient, so that the orthodontist may deform it into loops or a band fused onto a clasp, and must have the ability to return to its original shape. The wire must also be the most aesthetic, so that it does not disturb the looks of the human mouth. An ideal arch-wire with ideal properties does not exist.

Želene lastnosti ortodontskih žic so predvsem naslednje: dobra biokompatibilnost, dobra zaostala elastičnost, dobra povratna deformacija, žilavost in majhna lomljivost. Pomembno je tudi, da se žica lahko prožno oblikuje, ko jo ortodont deformira v zanko ali ko trak pritali na spono ter se potem vrne v prvotno obliko. Žica mora imeti tudi čim bolj estetski videz, tako da ne moti pogleda v človeška usta. Idealna žica za loke z idealnimi lastnostmi ne obstaja.

V zadnjih letih se je zlitina NiTi z oblikovnim spominom začela uporabljati v začetni fazi ortodontskega zdravljenja. Ta material se je uveljavil v ortodontski praksi zaradi svojih funkcionalnih mehanskih lastnosti. Prvič ga je leta 1975 uporabil v ortodontske namene dr. Andreasen z Univerze Iowu [4].

Vzrok, zakaj se je zlitina NiTi z oblikovnim spominom začela uporabljati v ortodontski praksi, je njena dobra biokompatibilnost in ker ima specifično mehansko lastnost, superelastičnost, ki jo imajo zlitine z oblikovnim spominom. Pomembna funkcionalna lastnost zlitin z oblikovnim spominom, ki se uporabljajo za ortodontske žice, je majhen modul elastičnosti, kar ustvarja majhno silo na zobe in veliko povratno deformacijo, dodatno pa vzdržuje konstantno silo med celotnim zdravljenjem. Te lastnosti so pomembne za ortodontsko popravo zob, kar uspešno izboljša superelastičnost zlitine NiTi z oblikovnim spominom [5].

V tem prispevku je predstavljena izdelava zlitine z oblikovnim spominom skupaj z rezultati temperaturnih meritev fazne premene, ki so bile narejene z diferencialno vrstično kalorimetrijo (DSC). Meritve modula elastičnosti in značilnega raztezka trgovsko dosegljivih ortodontskih žic za loke iz zlitin NiTi z oblikovnim spominom so prikazane grafično. Na koncu

In recent years SMA NiTi came into use in the initial stage of the orthodontic treatment. This material has been established in orthodontic practice because of its functional mechanical properties. For orthodontic purposes it was first introduced in 1975 by Dr. Andreasen of the University of Iowa [4].

The reason why the SMA NiTi was introduced into orthodontic practice is that it has good biocompatibility and has a specific mechanical property (superelasticity), which SMAs possess. An important feature of the functional SMA used for the orthodontic wire is the low modulus of elasticity, which creates a small force on the teeth and large recoverable strain (range), which, in turn, creates a continuous duration of force during orthodontic treatment. These properties are important in the process of orthodontic treatment and this improves the superelasticity of SMA NiTi successfully [5].

In the present work is presented SMA manufacture, together with the results of measuring the temperature of the phase transition with Differential Scanning Calorimetry (DSC). On the graphs we showed measurements of the modulus of elasticity and characteristic elongation on commercially available SMANiTi orthodontic arch-wire. At the end of the paper we showed the test of the biocompatibility of orthodontic wire.

## 2 Manufacture of Ni-Ti alloy

The chemical composition of the SMA NiTi is important because the properties are very sensitive to the initial chemistry. NiTi alloys have almost equiatomic composition. The chemical composition is very important in SMA because it has a decisive influence on the phase transitions temperature. The equiatomic composition (50 at.% Ni

je prikazan tudi biokompatibilnostni preskus ortodontske žice.

## 2 Izdelava zlitine NiTi

Kemična sestava zlitine NiTi z oblikovnim spominom je pomembna, ker so lastnosti zelo občutljive na začetno kemično sestavo. Zlitine NiTi imajo skoraj ekvatomsko sestavo. Kemična sestava je zelo pomembna pri zlitinah z oblikovnim spominom, ker odločilno vpliva na temperaturo fazne premene. Zlitina z ekvatomsko sestavo (50 at.% Ni in 50 at.% Ti) ima najvišjo temperaturo  $A_f$  120 °C. S povečevanjem deleža nikljevih atomov se temperatura premene znižuje. Pri 51 at. % je temperatura premene  $A_f$  – 40 °C [6].

Izdelava zlitine NiTi je zapletena. Slika 2 prikazuje shematično zaporedje postopkov [5,7]:

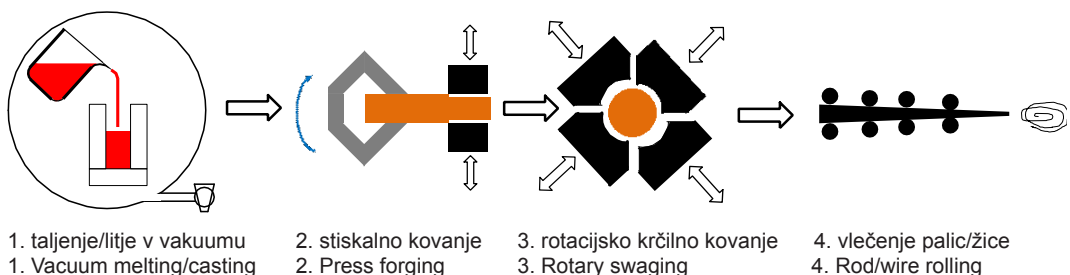
1. Taljenje/ulivanje v vakuumu: nikelj-aluminijeve zlitine se pogosto izdelujejo z indukcijskim taljenjem v vakuumu v grafitnem talilniku, ker je staljena zlitina NiTi zelo reaktivna, če je titana blizu petdeset odstotkov. Za indukcijsko taljenje v vakuumu se najraje uporablajo talilniki iz grafita ali CaO, ker drugi materiali onesnažijo staljeni NiTi s kisikom. Surovine se določijo, preden se zlitina stali z vakuumskim obločnim pretaljevanjem. Ta postopek se uporablja, ker omogoča najboljšo možno homogenost in čistost zlitine. Dvojno vakuumsko taljenje zagotavlja kakovost in doseganje mehanskih lastnosti zlitine.
2. Ingoti se vroče preoblikujejo s stiskalnim kovanjem.
3. Sledi rotacijsko krčilno kovanje do različnih oblik. Optimalna temperatura za vroče preoblikovanje je okoli 800 °C. Pri tej temperaturi je zlitina dobro preoblikovalna, niti se ne pojavlja

and 50 at.% Ti) exhibits the maximum  $A_f$  temperature 120 °C. By increasing the value of Ni atomic percentage, the transformation temperature decreases. For 51 at.% nickel it is  $A_f$  –40 °C [6].

Production of nickel-titanium is a complex process. Figure 2 shows a schematic view of the processes that occur after the following [5, 7]:

1. Vacuum melting/casting: Manufacture of nickel-titanium alloys is often done by Vacuum Induction Melting (VIM) in a graphite crucible. The reason we used VIM is because the molten state of NiTi is very reactive if Ti is close to fifty percent. The graphite or calcia (CaO) crucible is preferred for VIM because the others contaminate the molten NiTi with oxygen. The raw materials are formulated before the alloy is melted by Vacuum Arc Remelting (VAR). This VAR process takes place in order to achieve the best possible homogeneity and purity of the alloy. The double vacuum melting process ensures quality and maintains the mechanical properties of the alloy.
2. The ingots are hot worked with press forging.
3. Follow rotary swaging to different shapes. The optimal temperature for hot working appears to be around 800 °C. At this temperature the alloy is easily workable and there is not too severe oxidation of the surface.
4. Following cold worked on sizes (rolling) according to the product (rod, wire). Cold working of NiTi is complex because the alloy work-hardens rapidly.

The procedure (Figure 3) of hot and cold treatments, followed by the rolling procedure, obtained a tapered shape, followed by the procedure of annealing the wire or rod into a coiled state. Due to work-hardness it requires multiple reductions



**Slika 2.** Shematičen prikaz izdelavnega postopka za zlitino NiTi

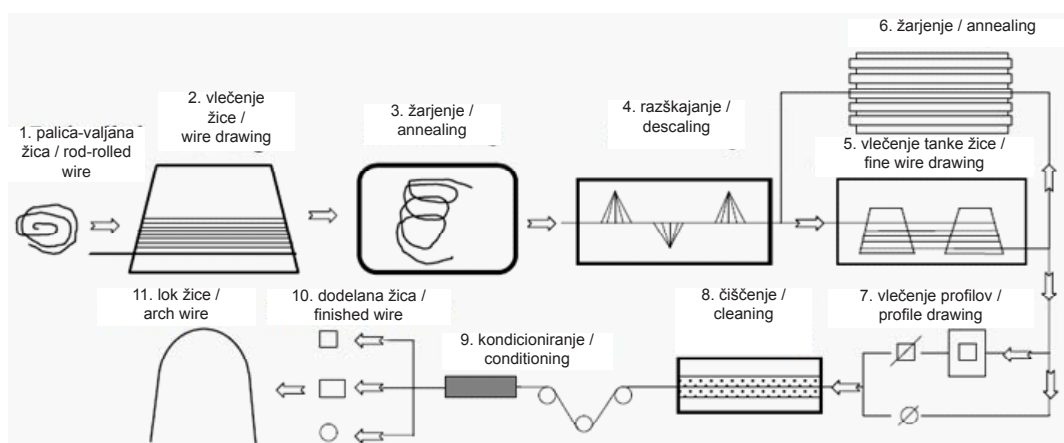
**Figure 2.** Schematic representation of the manufacturing process of NiTi alloy

močna oksidacija površine.

4. Sledi hladno preoblikovanje (*valjanje*) v končne oblike (palice, žica). Hladno preoblikovanje zlitine NiTi je zapleteno, ker se zlitina hitro preoblikovalno utrjuje.

Postopek (slika 3) je sestavljen iz vroče in hladne predelave, sledi valjanje žice, ki se navija na koničnem navjalniku, nato žarjenje debele ali tanke žice v zvitkih. Zaradi preoblikovalnega utrjevanja je pri valjanju potrebna redukcija v več stopnjah in pogosto medfazno žarjenje pri 600 – 800 °C. Sledi razškajanje in nato vlečenje tanke žice ter ponovno žarjenje. Po teh fazah predelave sledi izdelava končnih profilov (okroglo, kvadratno, pravokotno). Pravokotne žice se izdelujejo z vlečenjem okroglih žic. Zaradi velike povratne elastičnosti zlitine NiTi z oblikovnim spominom smo imeli nekaj težav pri vročem in hladnem preoblikovanju, ker je to zlitino težko oblikovati pri sobni temperaturi. Naslednji korak je bilo čiščenje žice, ki mu je sledilo učenje žice. Učenje je termomehanska obdelava, da se dosegajo optimalne lastnosti. Superelastični materiali NiTi se obdelujejo pri okoli 500 °C. Za zlitine z oblikovnim spominom je primerna temperatura v območju 350 – 400 °C. S strojno obdelavo se dobi končno obliko. Zlitina NiTi se lahko strojno obdeluje na standardne načine, kot je frezanje ali struženje, a je težava z obrabo orodja. Žice iz

and frequent inter-pass annealing at 600–800 °C. This is followed by the procedure of descaling, and then comes the process of fine drawing of wire and again annealing. After these phases follows the actual production profile (round, square, rectangular). The rectangular wires can be manufactured by drawing round wires. Due to the high spring-back of SMA NiTi we had some problems in hot and cold work as this alloy is difficult to form at an ambient temperature. The next step is then cleaning of the wire, followed by training of the wire. Training is thermo-mechanical treatment to achieve the optimized properties. Superelastic NiTi materials are heat treated in the vicinity of 500 °C. For shape memory alloys a suitable temperature is in the range between 350 °C and 450 °C. The machining is then made of the final profile. NiTi can be machined using conventional techniques such as milling, turning, but there are problems with tool wear. SMA NiTi wires we can be sheared and blanked quite effectively with proper tool design and maintenance. We can use this material successfully for abrasive processes such as grinding, sawing. This is important at the end of production for orthodontics; it is arch-wire [5, 7].



**Slika 3.** Shematičen prikaz izdelave končne NiTi-žice

**Figure 3.** Schematic representation of the production of finished NiTi wire

zlitine NiTi z oblikovnim spominom se lahko učinkovito režejo ali štančajo s primernim orodjem in njegovim vzdrževanjem. Lahko se tudi brusijo in žagajo. To je pomembno za izdelavo končnega ortodontskega izdelka, kar je žica za loke. [5,7].

### 3 Osnovni pojav

Zlitina NiTi kaže termoelastično martenzitno premeno. Ta premena povzroča pri zlitini ali oblikovni spomin ali superelastičnost.

#### 3.1 Oblikovni spomin

Izraz oblikovni spomin izvira iz edinstvene sposobnosti zlitin da se 'spomnijo' predhodno določene oblike: celo po močni deformaciji za več odstotkov so se zlitine sposobne spontano vrniti v prvotno, predhodno določeno obliko pri določenih topotnih razmerah. Za zlitino z oblikovnim spominom je značilno, da pri njej pri določeni temperaturi nastopi fazna premena. Te temperature prikazuje slika 4 in se jih lahko opiše na naslednji način: Temperatura  $M_s$  (začetek martenzitne premene) je

### 3 Basic phenomenon

NiTi alloy exhibits a thermoelastic martensitic transformation. This transformation is responsible for either shape memory or superelasticity being exhibited by the alloy.

#### 3.1 Shape memory

The term shape memory stems from its unique ability to 'memorize' predetermined shape(s): Even after severe deformation of several percent (strain), they are capable of returning spontaneously to their original or parent, pre-deformed shape under certain thermal conditions. SMA is characterized with the characteristic temperatures of phase transformation. These temperatures are presented in Figure 4 and described as follows. Temperature  $M_s$  (martensite-start) is the temperature at which the austenite cools down and begins to transform to martensite. Temperature  $M_f$  (martensite-finish) is the temperature at which the material has a complete twinned martensite. Temperature  $A_s$  (austenite-start) is the temperature at which martensite begins to change into austenite. Temperature  $A_f$

temperatura, pri kateri se avstenit ohladi in začne pretvarjati v martenzit. Temperatura  $M_t$  (konec martenzitne premene) je temperatura, pri kateri se je material v celoti pretvoril v martenzit. Temperatura  $A_s$  (začetek nastajanja avstenita) je temperatura, pri kateri se martenzit začenja spremenjati v avstenit. Temperatura  $A_f$  (konec nastajanja avstenita) je temperatura, pri kateri je končana pretvorba v avstenit [6].

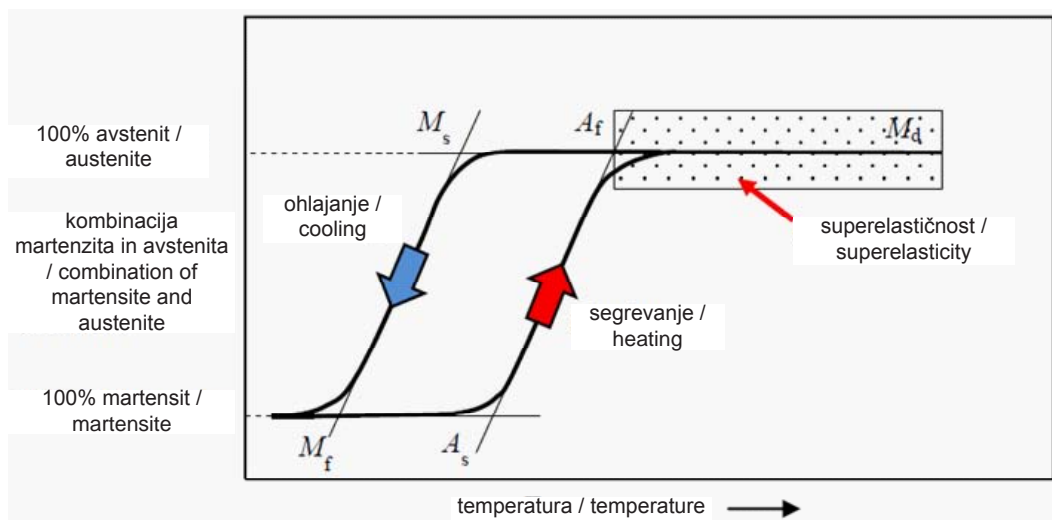
Pod temperaturo  $M_f$  se mikrostruktura zlitine z oblikovnim spominom pretvori iz avstenita s telesno centrirano kubično mrežo v martenzit z monoklinsko kristalno zgradbo (slika 5). Pod vplivom deformacije se zlitina z oblikovnim spominom pretvori v deformirani ali razdvojeni martenzit. S segrevanjem se lahko zlitina z oblikovnim spominom pri temperaturi nad temperaturo  $A_f$  vrne v prvotno fazo.

Slika 5 Makroskopska in mikroskopska predstavitev pojava oblikovnega spomina

(austenite-finish) is the temperature at which the transformation in the austenite phase is completed [6].

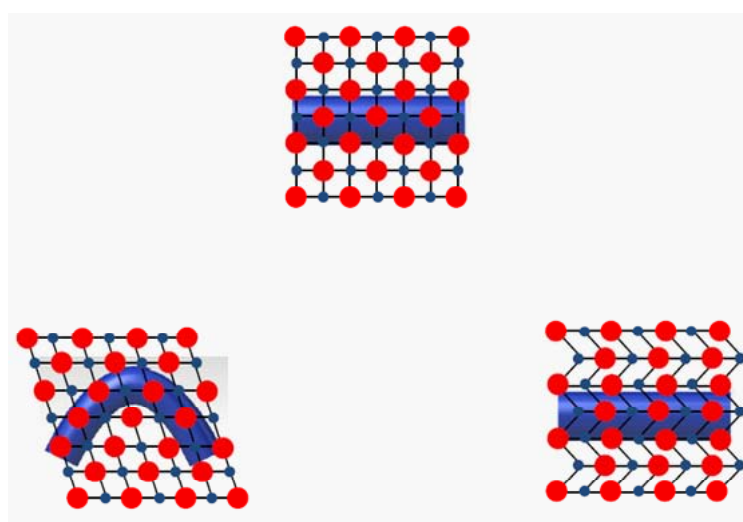
Under temperature  $M_f$  the structure of the SMA transforms from austenite with a body centered cubic (BCC) crystal structure to martensite with a monoclinic crystal structure (Figure 5). Under the influence of the deformation, the SMA deforms and transforms to deformed or detwinned martensite. By heating the SMA above the temperature  $A_f$  it can be returned to the original (parent) phase.

The natural characteristic of materials with shape memory is to memorize their shape before pseudo-plastic deformation in the austenite state (one-way), but not the shape which has been obtained by the deformation. This can be learned with training. Training is cyclic thermo-mechanical treatment. In the case of a two-way memory formative gives two conditions:



**Slika 4.** Histerezma martenzitne premene – zlitina z oblikovnim spominom se v temperaturnem območju od  $A_f$  do  $M_d$  obnaša superelastično

**Figure 4.** Hysteresis at martensitic transformation – SMA has, from the temperature  $A_f$  to  $M_d$ , superelasticity behaviour



**Slika 5.** Makroskopska in mikroskopska predstavitev pojava oblikovnega spomina

**Figure 5.** Macroscopic and microscopic presentation of shape memory effect

Naravna značilnost materialov z oblikovnim spominom je, da se spomnijo svoje oblike pred psevdoplastično deformacijo v avstenitno stanje (enosmerni spomin), ne pa oblike, ki je bila dosežena z deformacijo. To se lahko nauči z učenjem. Učenje je krožna termomehanska obdelava. Pri dvosmernem spominu je mikrostruktura, ki se pretvarja, lahko ali v martenzitnem stanju ali v avstenitnem stanju [6].

### 3.2 Superelastičnost

Superelastičnost je lastnost ali sposobnost materialov, ki so bili močno deformirani, za 6 – 10 %, da se po razbremenitvi vrnejo v prvotno stanje ali obliko [7]. Za superelastičnost je značilno, da nastopi, ko je material deformiran nad temperaturo  $A_f$  in zunanje napetosti povzročijo premeno osnovne avstenitne faze v martenzitno fazo (slika 6). Ta premena je brezdifuzijska premena v trdnem stanju iz kristalografsko višje urejene osnovne faze (telesno centrirani kubični avstenit) v kristalografsko nižje urejeno fazo (monoklinski martenzit) [8]. Premeno povzroči popačenje mreže

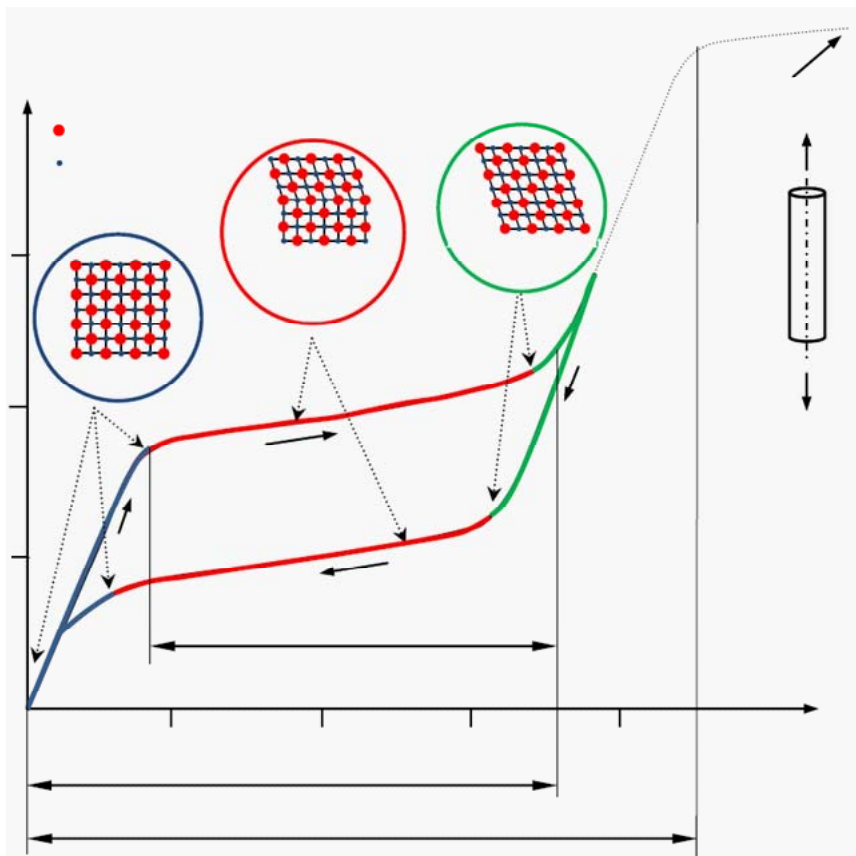
One in the martensitic state and the other in an austenitic state [6].

### 3.2 Superelasticity

Superelasticity is the property or ability of materials to return a very high strain of ~ 6-10% in the original position or shape spontaneously upon unloading (Figure 7). Superelasticity is caused typically when a material is deformed above  $A_f$ , where external applied stress induces the transformation of the parent austenite phase to a martensitic phase (Figure 6). This transformation takes place in the solid-solid diffusion-less phase transformation between the crystallographically more ordered parent phase (austenite (BCC)) and the crystallographically less ordered product phase (martensite (monoclinic)) [8]. Transformation caused the lattice distortion of the martensite from the austenite [9]. The austenite is the stable phase under stress-free conditions. In the case of application of a critical stress, the austenite yields and starts transformation to the martensite phase at a constant stress, thus producing a stress

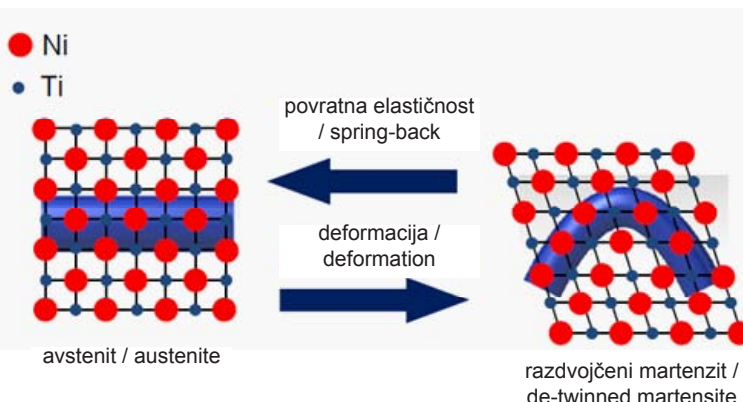
martenzita, nastalega iz avstenita [9]. Avstenit je stabilna faza v razmerah, ko ni napetosti. Če pa pride do kritičnih napetosti, avstenit popusti in se začne pri konstantni napetosti pretvarjati v martenzitno fazo tako, da nastane napetostna ploščad. Martenzit postane nestabilen, ko popustijo napetosti, zato se pri razbremenitvi martenzit ponovno pretvarja v avstenitno fazo in ko ni več nobene obremenitve, bi moral material imeti v celoti avstenitno zgradbo, tedaj vzorec dobi prvotno, nedeformirano obliko. Superelastičnost se pojavlja v temperaturnem območju  $A_f < T < M_d$  (slika 4).

plateau. The martensite becomes unstable upon the removal of the stress; hence, during unloading, the martensite phase reverse transforms to the austenite phase and, at zero loads, the material should be entirely austenitic with the specimen recovering its original undeformed shape. Superelasticity typically occurs in a temperature range between  $A_f < T < M_d$  (Figure 4).



**Slika 6.**  
Shematični  
prikaz pojave  
superelastičnosti  
(krivulja napetost  
– deformacija  
za zlitino z  
oblikovnim  
spominom  
pri enosni  
obremenitvi)

**Figure 6.**  
Schematic  
representation  
of superelastic  
effect (stress-  
strain curve  
for SMA under  
uniaxial loading).



**Slika 7.** Makroskopska in mikroskopska predstavitev superelastičnosti v zlitinah z oblikovnim spominom

**Figure 7.** Macroscopic and microscopic presentation of superelasticity in shape memory alloy

#### 4 Eksperimentalne meritve

##### 4.1 Meritve temperature $A_f$

V razmerah brez napetosti se temperature fazne premene navadno merijo z diferenčno vrstično kalorimetrijo (DSC). V naši raziskavi smo hoteli s to metodo ugotoviti temperaturo, pri kateri ima material (zlitina NiTi z oblikovnim spominom) popolnoma avstenitno mikrostrukturo in kaže superelastično obnašanje.

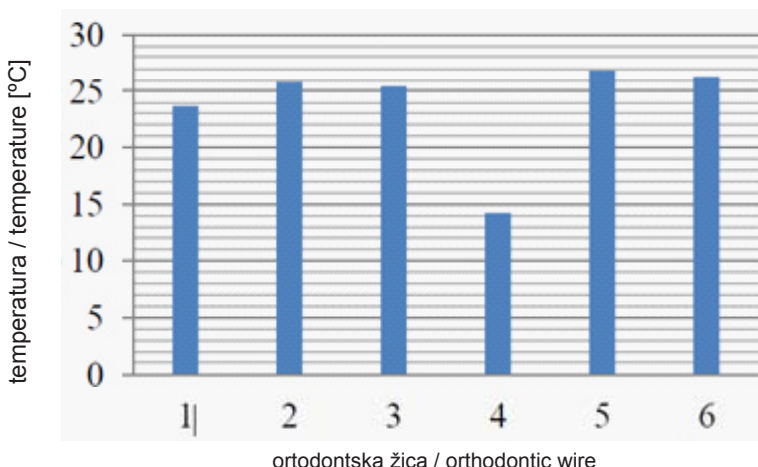
Pokazano je bilo, da imajo vse ortodontske žice temperaturo  $A_f$  pod telesno temperaturo. Temperature žic so

#### 4 Experimental measurements

##### 4.1 Measurements of $A_f$ temperature

Under stress free conditions the phase transition temperatures are measured commonly by DSC (Differential Scanning Calorimetry). In our research we wanted with this method to find a temperature at which the material (SMA NiTi) has fully austenitic microstructure and shows superelastic behaviour.

It has been shown that all the orthodontic wires have the temperature  $A_f$  below body temperature. Wire temperatures were

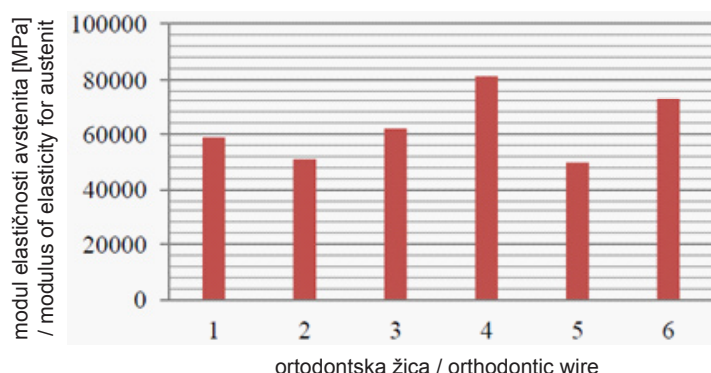


**Slika 8.** Temperatura  $A_f$  za različne ortodontske žice

**Figure 8.** Temperature  $A_f$  for different orthodontic wires

**Slika 9.** Elastični modul avstenita za različne ortodontske žice.

**Figure 9.** Elastic modulus of austenite for different orthodontic wires



bile ugotovljene med 14 °C in 26 °C in to je prikazano na sliki 8. Deformacijska ploščad je močno odvisna od temperature  $A_f$ . Zato je temperatura  $A_f$  zlitine NiTi z oblikovnim spominom zelo pomembna pri vseh medicinskih uporabah.

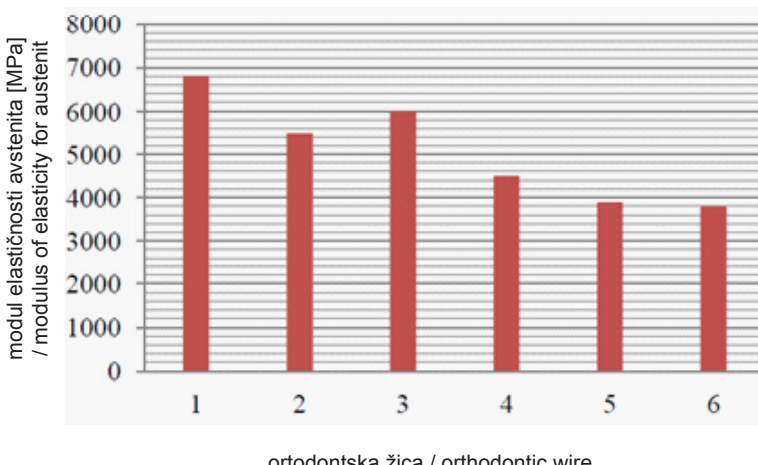
#### 4.2 Meritve mehanskih lastnosti

Mehanske lastnosti zlitin z oblikovnim spominom so močno odvisne od temperature  $A_f$ . Naslednja razpredelnica kaže mehanske lastnosti ortodontskih žic iz zlitine NiTi z oblikovnim spominom, ugotovljenih z enoosnim nateznim preskusom. Za natezne preskuse smo uporabili stroj Zwick/Roell

analysed from 14 °C to 26 °C and are shown in Figure 8. The transformation plateau is highly dependent on the  $A_f$  temperature. Therefore, the  $A_f$  temperature of the SMA NiTi is very important in all medical applications.

#### 4.2 Measurement of mechanical properties

The mechanical properties of SMA are largely dependent on the temperature  $A_f$ . The following Table shows the mechanical properties of SMA NiTi orthodontic wires obtained from the uniaxial tensile test. The tensile tests were performed using a Zwick/



**Slika 10.** Elastični moduli različnih ortodontskih žic na premembni ploščadi

**Figure 10.** Elastic modulus of transformation plateau for different orthodontic wires

ZO 10. Krivulja napetost – deformacija pri statičnem nateznem preskusu je odvisna od mikrostrukture (avstenit, premena ali martenzit). Slika 9 kaže naklon začetnega dela obremenitvene krivulje (elastični modul avstenita). Moduli elastičnosti za avstenit so v območju 50 000 – 81 000 MPa.

Nasliki 10 je prikazan naklon premembne faze ali območja  $E_2$  (prehod avstenita v martenzit) za različne ortodontske žice. Moduli elastičnosti za območje premene so med 4500 MPa in 6800 MPa.

Na sliki 11 je prikazan naklon zadnjega dela krivulje  $E_3$  (elastični moduli martenzita) za različne ortodontske žice. Moduli elastičnosti martenzita so v območju 32 500 – 50 000 MPa.

Na sliki 12 so prikazani raztezki različnih ortodontskih žic na premembni ploščadi,  $l_t$ . Raztezki so v območju 5 – 7 %.

Na sliki 13 so prikazani raztezki  $l_s$  superelastičnosti za različne ortodontske žice. Ti raztezki so v območju 6 – 8 %. Ta podatek je zelo pomemben za ortodontsko žico, da deformacija pri ortodontski obdelavi ne preseže tega območja.

Na sliki 14 so prikazani raztezki povratne elastičnosti  $l_{sb}$  za različne ortodontske žice. To pomeni stopnjo, do katere se aktivirana žica loka vrne v prvotno stanje po dezaktiviranju [10]. Ti so v območju 10 –

Roell ZO 10. The stress-strain curve from a static tensile test depends on microstructure (austenite, transformation or martensite).

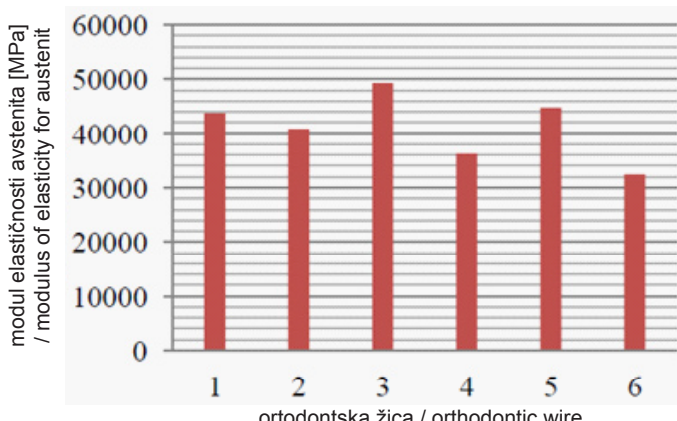
In Figure 9 are presented the slope of the initial part of the loading curve (elastic modulus of austenite). Modules of elasticity for austenite are in the range from 50000 to 81000 MPa.

Figure 10 presents the slope of the transformation phase or region  $E_2$  (austenite to martensite) for different orthodontic wires. Modules of elasticity for the transformation region are in range from 4500 to 6800 MPa.

Figure 11 presents the slope of the final part of the curve  $E_3$  (elastic modules of martensite) for different orthodontic wires. Modules of elasticity for martensite are in the range from 32500 to 50000 MPa.

Figure 12 presents the elongations of transformation plateau  $l_t$  for different orthodontic wires. These elongations are in the range from 5 to 7 %.

Figure 13 presents  $l_s$  the elongation of superelasticity for different orthodontic wires. These elongations are in the range from 6 to 8 %. This information is very important in orthodontic wire, because deformation in orthodontic treatment does not exceed this range.

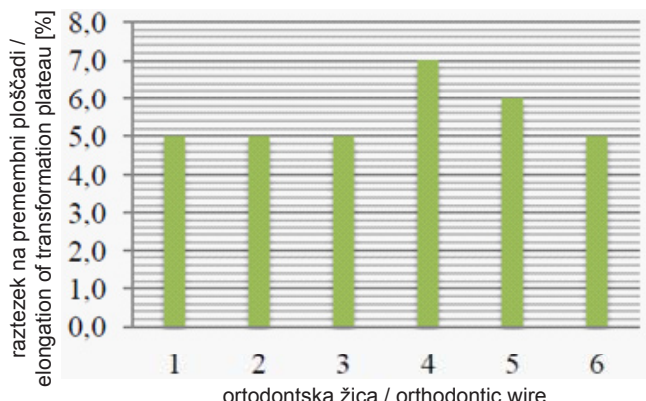


**Slika 11.** Elastični modul martenzita za različne ortodontske žice

**Figure 11.** Elastic modulus of martensite for different orthodontic wires

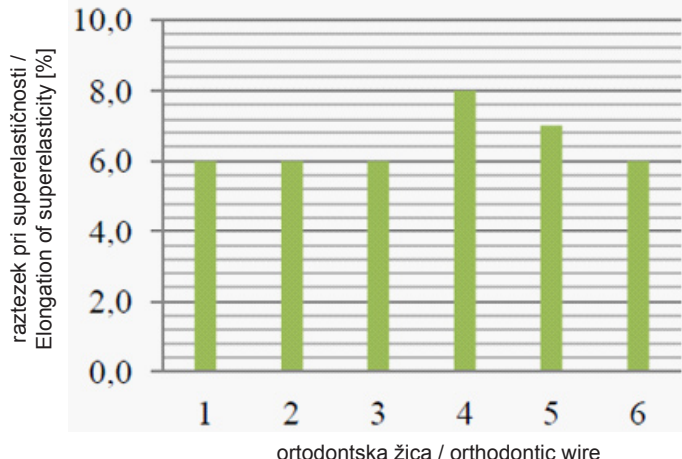
**Slika 12.** Raztezki različnih ortodontskih žic na premembni ploščadi

**Figure 12.** Elongation of transformation plateau for different orthodontic wires



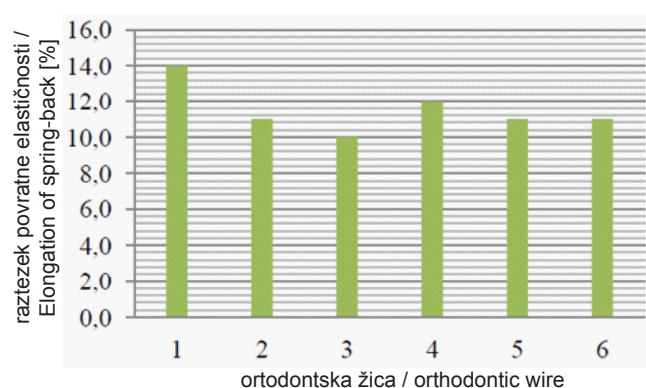
**Slika 13.** Raztezek pri superelastičnosti za različne ortodontske žice

**Figure 13.** Elongation of superelasticity for different orthodontic wires



**Slika 14.** Raztezek povratne elastičnosti za različne ortodontske žice

**Figure 14.** Elongation of spring-back for different orthodontic wires



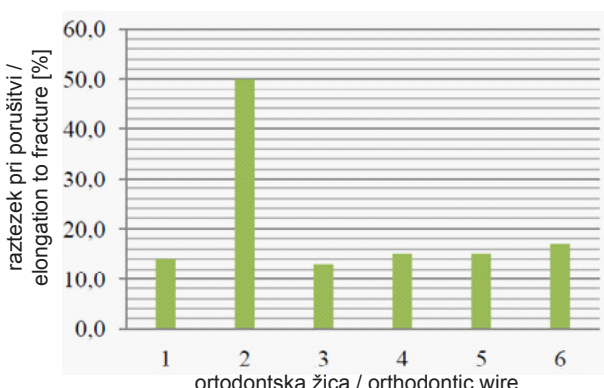
14 %. Ta podatek je pomemben, da se zna načrtovati sestavine za različne uporabe.

Slika 15 prikazuje raztezke pri porušitvi,  $I_f$ , ortodontskih žic. Ti raztezki so v območju

Figure 14 presents the elongations of spring back  $I_{sb}$  for different orthodontic wires. This means the extent to which the range recovers upon deactivation of an activated

**Slika 15.** Raztezki pri porušitvi za različne ortodontske žice

**Figure 15.** Elongation to fracture for different orthodontic wires



13 – 50 %. Ortodontska žica 2 je imela za razliko od ostalih 50 %-ni raztezek.

## 5 Biokompatibilnost

Splošnoprvzetadefinicijabiokompatibilnosti je zelo zapletena. Williams (1988) je biokompatibilnost opisal kot »sposobnost materiala, da deluje s primernim odzivom gostitelja pri določeni uporabi«. Ta definicija pokrije dejstvo, da je možnih veliko interakcij med biomaterialom in gostiteljem ter da se ne osredotoča samo na učinke zastrupitve ali poškodbe gostiteljevega sistema. Bolj konkretno definicijo je leta 1998 predlagal Wintermantel, kjer biokompatibilnost definiral kot strukturno in površinsko kompatibilnost med tehničnim in biološkim sistemom, kjer strukturni del določajo mehanske lastnosti, površinsko kompatibilnost pa določajo površinske fizikalne, kemične, biološke in morfološke lastnosti biomateriale. Danes je potrebno biokompatibilnost vrednotiti z ustreznimi standardi [11].

### 5.1 Vpliv kemičnih elementov niklja in titana

Titan se smatra kot zelo biokompatibilen. Na drugi strani je nikelj biokompatibilen in strupen. Nikelj je zelo močan alergen

arch-wire [10]. This size is in the range from 10 to 14 %. This information is important so as to know the design components for a variety of applications.

Figure 15 presents the elongations to fracture  $\ell_f$  of orthodontic wires. These elongations are in the range from 13 to 50 %. Orthodontic wire 2 has, unlike the others, 50% of elongation to fracture.

## 5 Biocompatibility

The generally accepted definition of biocompatibility is very complicated. Williams (1988) described biocompatibility as “the ability of a material to perform with appropriate host response in a specific application”. This definition covers the fact that there are a variety of interactions possible between biomaterial and the host, and it does not focus solely on toxicity or injurious effects to the host system. A more concrete definition was proposed in 1998 by Wintermantel, who defined biocompatibility as the structural and surface compatibility between a technical and a biological system, where the structural part is governed by the mechanical properties, and the surface compatibility by the biomaterial's superficial physical, chemical, biological and morphological properties. Today, it is

in povzroča zelo občutljivo reakcijo v večji meri kot katerakoli kovina ali zlitina. Kovinski nikelj, nikljev sulfid, nikljev oksid in nikljev karbonat so za človeka zanesljivo karcerogeni [12].

## 5.2 Zaščitna plast TiO<sub>2</sub>

Titan in njegove zlitine lahko nastanejo na zunanji površini filma titanovega oksida (TiO<sub>2</sub>) z majhnim deležem NiO. Zaradi sposobnosti tvorbe plasti stabilnega titanovega oksida je titan eden od najbolj biokompatibilnih materialov. V najugodnejših razmerah, ki predstavljajo izvrstno osteo integracijo s kostjo, je tudi sposobnost tvorbe kalcijevega fosfata na površini, ki tudi preprečuje korozijo. Druga koristna lastnost je, da se v primeru poškodbe zaščitne plasti, predvsem titanovega oksida in kalcijevega fosfata, ta plast regenerira [13].

Cilj prve faze ocene biokompatibilnosti žice iz Ni-Ti je preiskava možne citotoksičnosti ortodontskih žic iz Ni-Ti na modelu podganjih timocitov, kjer se ustvari neposreden stik med materialom in celicami.

Ta preskus je bil izbran zato, ker je velika občutljivost timocitov na pro-apoptotične dražljaje in preskus vključuje kulture celic, ki se ne zraščajo in ne razmnožujejo, kot so timociti, in je mnogo primernejši za oceno citotoksičnosti materiala v neposrednem stiku v primerjavi z zraščenimi celicami, kot so fibroblasti.

Poskus je bil pripravljen tako, da se je pripravilo gojišče podganjih timocitov z vloženimi vzorci Ni-Ti-žice pri različnih razmerjih površina-prostornina žic v celotnem mediju. Citotoksični učinek se je ocenjeval z meritvami apoptoze.

Timociti so bili izolirani iz timusov (prijevljcev) moških podgan albino oxford (AO), starih 2-2 in pol mesecev. Vse študije na živalih je odobril odbor za etiko inštituta

necessary to evaluate the biocompatibility in accordance with the relevant Standard [11].

## 5.1 The influence of the chemical elements nickel and titanium

Titan is classified as highly biocompatible. On the contrary, the nickel is biocompatible and toxic. Nickel is a very strong allergen and causes a very sensitive reaction to a greater extent than any metal or alloy. Nickel metal, nickel sulphide, nickel oxide and nickel carbonate are definitely human carcinogens [12].

## 5.2 Protective layer of TiO<sub>2</sub>

The titanium and its alloys can be formed on the outer surface of the film of titanium oxide (TiO<sub>2</sub>) with a small amount of NiO. Due to the ability to form a stable titanium oxide layer on the surface, this is one of the most biocompatible materials. In the optimum condition, which can be an excellent osteo-integration with the bone, there is also the ability to form calcium phosphate on the surface, which also prevents corrosion. Another useful property is that, in the event of damage to the protective layer, in particular titanium oxide and calcium phosphate, the layer can be regenerated [13].

The aim of the first phase of biocompatibility assessment of Ni-Ti wire was to investigate the potential cytotoxicity of Ni-Ti orthodontic wires on a model of rat thymocytes, where a direct contact exists between the material and the cells.

The test was chosen because of the high sensitivity of thymocytes to pro-apoptotic stimuli and because the test includes the culture of non-adherent, non-proliferating cells, such as thymocytes, which is much more convenient for the evaluation of a material's cytotoxicity in direct contact,

za medicinske raziskave v skladu z navodili in priporočili EU za varovanje laboratorijskih živali. Po evtanaziji živali v etru se je kirurško s skalpelom odstranil timus in sosednje tkivo okoli timusa. Timus se je potem homogeniziral v najlonski mrežici s sponko v obliki brizge in suspenzija celic se je pripravila v RPMI-mediju. Sledilo je filtriranje in izpiranje suspenzije celic s centrifugo z 1400 obr./min 8 minut. Kepica celic se je ponovno suspendirala v popolnem RPMI-mediju, ki je bil sestavljen iz 10 % seruma iz plodu telička (FCS), 2-merkaptoetanola (200 µM) in antibiotikov (gentamicin, penicillin in streptomycin, 1 % raztopina). Preživetje celic po taki izolaciji je bila vedno večje od 95 %, kot ugotovljeno z obarvanjem celic z raztopino Trypan modro.

### 5.3 Priprava Ni-Ti-žic za biokompatibilnostne preskuse

Ni-Ti-žice (0,46 mm x 0,76 mm x 1000 mm), s površino 0,25 cm<sup>2</sup> za posamezno žico, so bile oprane v sterilni vodi in obdelane z ultrazvokom 10 minut pri sobni temperaturi. Vodna raztopina je bila potem zamenjana z 50 %-nim etilnim alkoholom in sledila je nadaljnja 15-minutna obdelava z ultrazvokom. Končno smo to raztopino zamenjali z 96 %-nim alkoholom in vzorce znova obdelovali 15 minut z ultrazvokom. Nato smo vzorce dali z diamantno pinceto v petrijevke, izpostavili laminarnemu toku zraka in za 10 ur UV-svetlobi. Tako sterilizirane vzorce ortodontnih žic iz Ni-Ti smo uporabili za preskuse biokompatibilnosti in kondicioniranja.

### 5.4 Gojenje timocitov in razmere za kondicioniranje

Timocite ( $4 \times 10^6$  celic na petrijevko) smo gojili v 24 petrijevkah v popolnem RPMI-mediju (500 µl na petrijevko) ali same ali s

compared to the adherent cells such as fibroblasts.

The experiment was designed to cultivate the Ni-Ti wire samples with rat thymocytes, using different surface-over-volume ratios of the wires in complete medium. The cytotoxic effect was evaluated by measuring the apoptosis.

Thymocytes were isolated from the thymuses of Albino oxford (AO) male rats, 2-2.5 months old. All studies on animals were approved by the Ethics Committee of the Institute for Medical Research, which subjugates the EU Guidelines and Recommendations on Laboratory Animal Welfare. Following the euthanasia of animals in ether and the surgical extraction of the thymus, the connective tissue around the thymus was removed using a scalpel. The thymus was then homogenized over a nylon mesh with a syringe clip and the cell suspension was made in basic RPMI medium. This was followed by filtration and washing of the cell suspension by centrifugation at 1400 rpm for 8 minutes. The cell pellet was re-suspended in complete RPMI medium, which consisted of 10% foetal calf serum (FCS), 2-mercaptopethanol (200 µM) and antibiotics (gentamicin, penicillin and streptomycin, 1% solution). The cells' viability after such isolation was always higher than 95%, as determined by staining the cells with Trypan blue solution.

### 5.3 Preparation of Ni-Ti wires for biocompatibility tests

Ni-Ti wires (0.46 x 0.76 x 1000 mm) with the surface of 0.25 cm<sup>2</sup> per wire were washed in sterile water and sonified at room temperature for 10 minutes. The aqueous solution was then replaced with 50% ethyl alcohol and the sonification continued for another 15 minutes. Finally, the solution was

prisotnimi ortodontskimi žicami. Ali pa smo celice gojili skupaj s steklenimi paličicami, ki niso bile citotoksične, kot smo preverili predhodno. Površina vzorcev orto Ni-Ti v celotni prostornini gojitvenega medija (razmerje površina-prostornina) se je gibala od 0,5 cm<sup>2</sup>/ml do 12,0 cm<sup>2</sup>/ml. Celice so se gojile pri 37 °C in 5 % CO<sub>2</sub> 24 ur, nato smo napravili citotoksične preskuse.

Ortodotske žice iz Ni-Ti smo kondicionirali v 3 ml popolnega RPMI-medija v 6 petrijevkah. Površina žice glede na prostornino medija je bila 3 cm<sup>2</sup>/ml. Po 7 dneh kondicioniranja smo medije zbrali in jih med prenosom vzorcev na analizo zamrznili pri -20 °C. Vzorce Ni-Ti smo prekrili z enako prostornino svežega medija. Da bi ugotovili učinke kondicioniranega medija na površinskomikrostrukturo Ni-Ti-vzorcev smo žice zbrali po 7 dneh kondicioniranja in jih 10 minut prali z ultrazvokom v sterilni vodi in nato sušili v laminarnem toku ter jih shranili v sterilnih Eppendorfovih epruvetah. Drugi del vzorcev je bil shranjen v Eppendorfovih epruvetah brez predhodnega splakovanja.

## 5.5 Ocene citotoksičnosti

Po 24 h smo z morfološko metodo ugotavljali apoptozo timocitov, ki so bili gojeni v prisotnosti ortodontskih žic iz Ni-Ti, s tem, da smo celice obarvali s Turkovo raztopino. Apoptotične celice smo ugotovili na osnovi njihovega homogeno obarvanega heterokromatina in delež apoptotičnih celic smo izračunali na osnovi vsaj 500 celic.

Dodatno smo ugotavljali apoptozo timocitov, gojenih v prisotnosti Ni-Ti-žic, s pretočno citometrijo, ko smo celice označili s propidijevim jodidom (PI), raztopljenim v hipotonični raztopini. Analizo smo naredili s pretočnim citometrom EPICS XL-MCL (Coulter, Krefeld, Nemčija) z 488 nm vzbujalnim laserjem. Med analizo je bil prehod timocitov krmiljen glede na njihovo

replaced with 96% alcohol, and the samples were sonified for another 15 minutes. The samples were then placed on Petri dishes using diamond tweezers, placed under a laminar air flow and exposed to UV light for 2-10 hours. The sterilized samples of Ni-Ti Orthodontic wires were then used in the tests of biocompatibility and conditioning.

## 5.4 Cultivation of thymocytes and terms of conditioning

Thymocytes ( $4 \times 10^6$  cells/well) were cultured in a 24-well plate in complete RPMI medium (500 ul/well), either alone, or in the presence of orthodontic Ni-Ti samples. Alternatively, the cells were cultivated with control glass rods, which are not cytotoxic, as we found previously. The area of Ortho Ni-Ti samples in the total volume of the culture medium (surface-to-volume ratio) ranged from 0.5 cm<sup>2</sup>/ml to 12.0 cm<sup>2</sup>/ml. The cells were cultured at 37 °C and 5% CO<sub>2</sub> for 24 hours, after which cytotoxicity tests were carried out.

Ni-Ti orthodontic wires were conditioned in 3 ml of complete RPMI medium in 6-wells plates. The surface of alloy over the volume of medium was 3cm<sup>2</sup>/ml. After 7 days of conditioning the media were collected and frozen at -20 °C, until the transportation of samples for the analysis. The other Ni-Ti samples were covered with the same volume of fresh medium. In order to determine the effects of conditioned medium on the surface microstructure of Ni-Ti samples, the wires were collected after 7 days of conditioning and washed by sonification in sterile water for 10 minutes, followed by drying in a laminar flow and preservation in sterile Eppendorf tubes. The second part of the samples was preserved in Eppendorf tubes without prior rinsing.

velikost in zrnavost z računalniškim programom na osnovi diagrama FS x SS, narejenega v SISTEMU II™. Dodatno analizo smo napravili s programom FlowJo. Rezultati iz pretočnega citometra so predstavljeni grafično, prikazujejo apoptočne celice, ki so bile označene kot celice z manjšo fluorescenco in primerjane z živimi celicami, glede na zavrnjeni genetski material. Raven nespecifične fluorescencije je bila ugotovljena z vzorci, ki niso bili obarvani z PI.

### 5.6 Učinek Ni-Ti žic na citotoksičnost in vitro

Te študije smo izbrali, ker so timociti (nedozoreli timični T-limfociti) občutljivi za apoptočne signale in vitro in glede na literaturne podatke o pro-apoptočnem učinku Ni-ionov. Uporabili smo najmanjše ( $0,5 \text{ cm}^2/\text{ml}$ ) in največje ( $6,0 \text{ cm}^2/\text{ml}$ ) razmerje med površino zlitine in prostornino medija s celično kulturo pri analizi z neposrednim stikom med celicami in materialom. Kot negativne primerjalne vzorce smo uporabili vzorce laboratorijskih steklenih paličic,



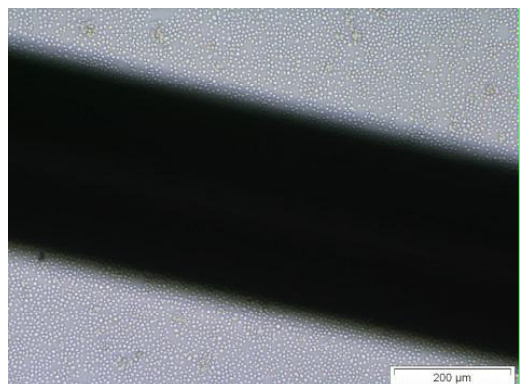
**Slika 16** Prikaz timocitov, ki so bili gojeni 24 h v popolnem gojitvenem mediju

**Figure 16.** The appearance of control thymocytes cultivated for 24 h in complete culture medium.

### 5.5 Cytotoxicity assays

After 24 h cultivation, the apoptosis of thymocytes cultivated in the presence of Ni-Ti orthodontic wires was determined using the morphological method, by staining the cells with Turk solution. Apoptotic cells were detected on the basis of their homogeneously stained heterochromatin, and the percentage of apoptotic cells was calculated on the basis of at least 500 cells.

Additionally, the apoptosis of thymocytes cultivated in the presence of Ni-Ti wires was determined using flow cytometry, upon labelling the cells with propidium iodide (PI) dissolved in hypotonic solution. The analysis was performed on the flow cytometer EPICS XL-MCL (Coulter, Krefeld, Germany) using a 488 nm excitation laser. During the analysis, thymocytes were gated based on their size and granularity, using the FS x SS diagram created in the SYSTEM II™ software programme. Subsequent analysis was performed using FlowJo software. The



**Slika 17.** Prikaz timocitov, ki so bili gojeni 24 h v popolnem gojitvenem mediju ob prisotnosti Ni-Ti-vzorcev

**Figure 17.** The appearance of thymocytes cultivated for 24 h in complete culture medium in the presence of Ni-Ti samples

obdelanih z raztopino deksametazona, ki je poznan po svojem farmakološkem uravnavanju apoptoze. Pojav kultur timocitov v prisotnosti ortodontskih žic iz Ni-Ti prikazujeta sliki 16 in 17.

Rezultati, ki se nanašajo na morfološko analizo, so prikazani na sliki 18.

Po 24 h je bilo gojišče z Ni-Ti-žicami ali paličicami za primerjanje in timociti obarvano s Turkovo raztopino in preiskano s svetlobno mikroskopijo. Apoptotične celice se je ugotovilo s homogeno obarvanim heterokromatinom, medtem ko je bil delež apoptotičnih celic izračunan na osnovi analize vsaj 500 celic. Rezultati so pokazali, da je bila srednja vrednost  $\pm SD$  ( $n = 5$ ) pri enem od reprezentativnih poskusov  $*p < 0,05$ ,  $***p < 0,05$  v primerjavi z ustrezнимi primerjalnimi vzorci (primerjalne steklene paličice).

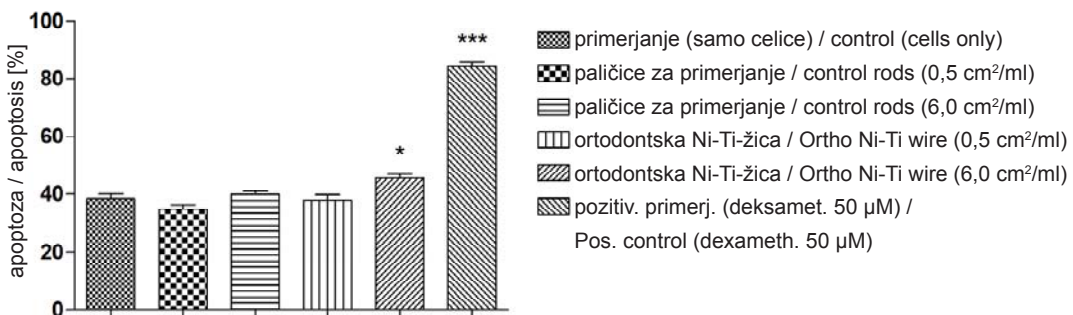
Sorazmerno velik delež apostoze je bil ugotovljen v gojišču, ki ni bilo občutno spremenjeno ali z negativnimi primerjalnimi vzorci ali zaradi vpliva vzorcev Ni-Ti ortodontskih žic z manjšo površino ( $0,5 \text{ cm}^2/\text{ml}$ ). A Ni-Ti žice z večjo površino so v enaki prostornini medija ( $6,0 \text{ cm}^2/\text{ml}$ ) občutno povečale apoptozo. Odstotek apoptotičnih timocitov je bil občutno manjši v primerjavi s pozitivnimi primerjalnimi vzorci in ta učinek

results from the flow cytometry are presented graphically, showing the apoptotic cells that were marked as the cells with a lower fluorescence compared to the live cells, due to their discarded genetic material. The level of nonspecific fluorescence was determined based on the samples that were not stained with PI.

### 5.6 The effect of Ni-Ti wires on cytotoxicity in vitro

These studies were chosen because of the sensitivity of thymocytes (immature thymic T lymphocytes) to apoptotic signals in vitro and literature data on the pro-apoptotic effect of Ni ions. We used the lowest ( $0.5 \text{ cm}^2/\text{ml}$ ) and the highest ( $6.0 \text{ cm}^2/\text{ml}$ ) alloys' surface-to-volume ratio in cell culture medium, in an assay of direct contact between the cells and the material. As a negative control we used the samples of laboratory glass rods with the same surface-to-volume ratio, whereas positive control samples were treated with a dexamethasone solution, which is known for its pharmacological modulation of apoptosis. The appearance of the thymocytes' cultures with Ni-Ti orthodontic wires, or control cultures is shown in Figures 16 and 17.

The results considering morphological analysis are presented in Figure 18.



**Slika 18** Morfološka analiza apoptoze timocitov v gojišču skupaj z Ni-Ti-zlitinami

**Figure 18.** Morphological analysis of thymocytes' apoptosis in culture with Ni-Ti alloys

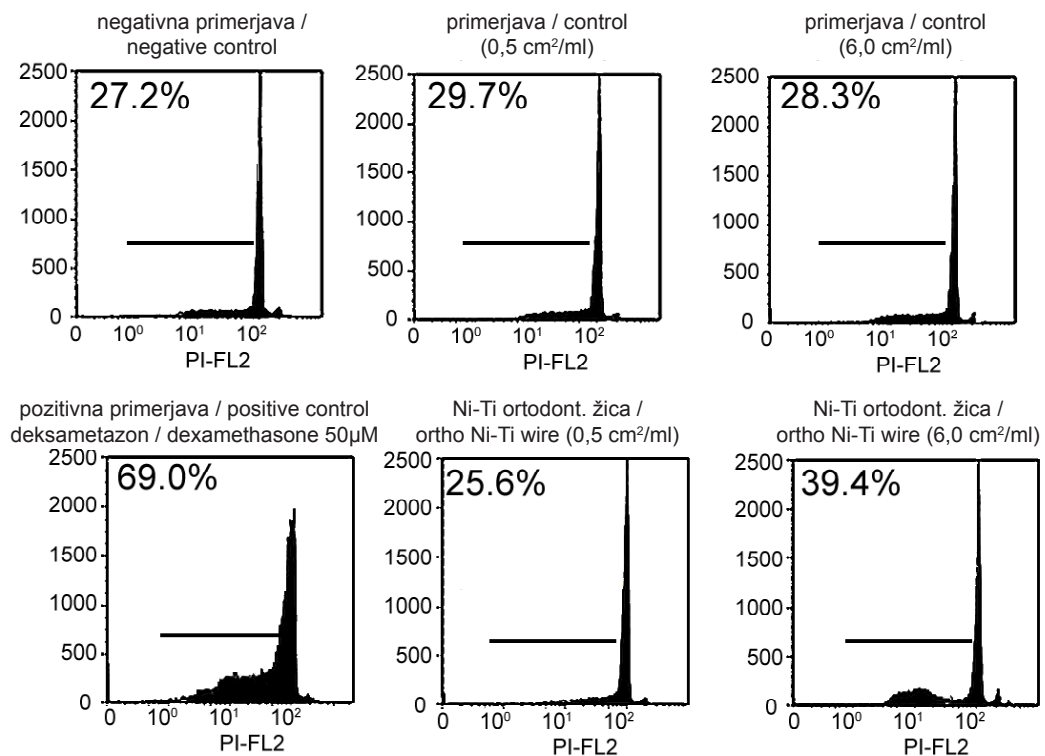
se lahko opiše kot šibek pri ocenjevanju po lestvici šibko – zmerno – močno.

Podoben pro-apoptotični učinek Ni-Ti-žic je bil potrjen pri drugi analizi apoptoze timocitov z obarvanjem joder s propidijevim jodidom. Slika 19 prikazuje reprezentativni preskus, medtem ko slika 20 kaže srednjo vrednost treh poskusov. Rahlo manjši odstotek celic s hipodiploidnimi jedri je v soglasju z že opisanim mehanizmom dinamičnega razvoja apoptoze v gojišču celic.

Po 24 h (Fig 19) je bilo gojišče timocitov skupaj z Ni-Ti-žicami ali primerjalnimi paličicami obarvano s propidijevim jodidom in analizirano s pretočnim citometrom. Apoptotične celice se je ugotavljalo na osnovi manjše količine genetskega materiala in s tem manjše intenzivnosti fluorescence

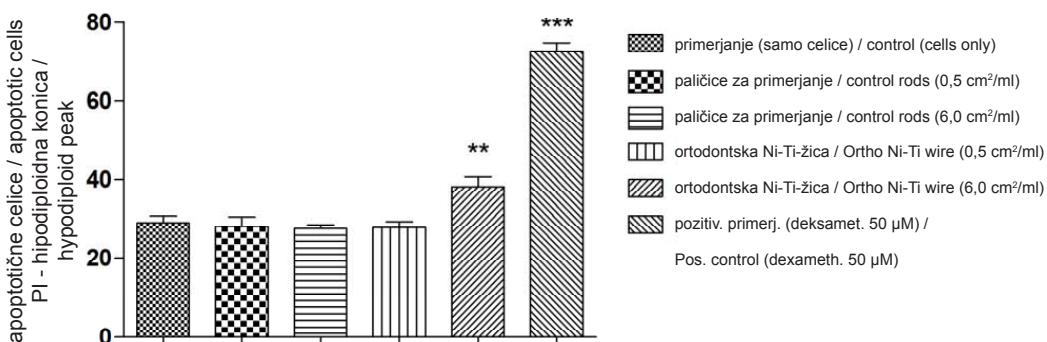
After 24 h – culture with Ni-Ti wires or control rods, thymocytes were stained using Turk solution and analysed by light microscopy. Apoptotic cells were detected on the basis of homogenously stained heterochromatin, whereas the percentage of apoptotic cells was calculated by analysing at least 500 cells. The results are shown as mean  $\pm$  SD ( $n = 5$ ) from one representative experiment. \* $p < 0.05$ , \*\*\* $p < 0.005$ , compared to corresponding control samples (control glass rods).

There was a relatively high rate of apoptosis in the culture, which was not modified significantly either by the negative control samples nor by the influence of orthodontic Ni-Ti samples of smaller surface area ( $0.5 \text{ cm}^2 / \text{ml}$ ). However, the larger surface of Ni-Ti wires that was placed



Slika 19. Analiza apoptoze timocitov v gojišču skupaj z Ni-Ti žicami s pretočnim citometrom.

Figure 19. Analysis of thymocytes' apoptosis in culture with Ni-Ti alloys by flow cytometry.



**Slika 20.** Analiza apoptoze timocitov v gojišču skupaj z Ni-Ti žicami s pretočnim citometrom

**Figure 20.** Analysis of thymocytes' apoptosis in culture with Ni-Ti alloys by flow cytometry

kot hipodiploidne celice. Reprezentativni histogram predstavlja en reprezentativni poskus.

Po 24 h je bilo gojišče timocitov skupaj z Ni-Ti-žicami ali primerjalnimi paličicami obarvano s propidijevim jodidom in analizirano s pretočnim citometrom. Apoptotične celice se je ugotavljalo na osnovi manjše količine genetskega materiala in s tem manjše intenzivnosti fluorescence kot hipodiploidne celice. Rezultati so prikazani kot srednja vrednost  $\pm$  SD treh poskusov  $^{**}p<0,01$ ,  $^{***}p<0,05$ , v primerjavi z ustreznimi primerjalnimi vzorci (primerjalne steklene paličice).

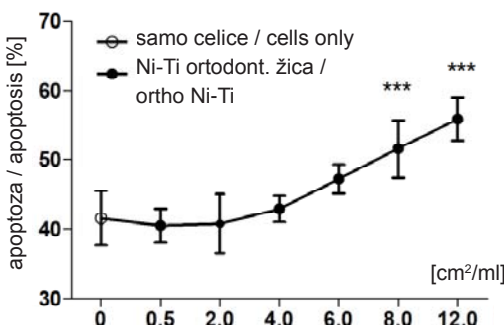
V drugem poskusu smo preiskovali v odvisnosti od doziranja učinek Ni-Ti ortodontskih žic na apoptozo podganjih timocitov v gojišču. Rezultate prikazuje slika 21. Vidi se, da je v okviru razmerja površina – prostornina biomateriala v mediju, ki ga priporočajo standardi ISO (0,5 – 6 cm<sup>2</sup>/ ml) samo večja količina Ni-Ti-žic povečala apoptozo timocitov, kar je občutno več kot pri spontani hipoptozi v gojišču. Količina Ni-Ti-žic, ki je bila večja od priporočene (8,0 cm<sup>2</sup>/ ml in 12,0 cm<sup>2</sup>/ml) je še dodatno povečala apoptozo vendar brez večje odvisnosti od doziranja.

in the same volume of medium (6.0 cm<sup>2</sup>/ ml) increased apoptosis significantly. The percentage of apoptotic thymocytes was lower significantly compared to the positive control, and this effect can be assessed based on the weak-moderate-strong scale, as a weak one.

A similar pro-apoptotic effect of Ni-Ti wires was confirmed in another assay of thymocytes' apoptosis, by staining the nuclei with propidium iodide. Figure 19 shows a representative experiment, whereas Figure 20 shows the mean of three experiments. The slightly lower percentage of cells with hypodiploid nuclei is in line with the already described mechanism of dynamic development of apoptosis in cell culture.

After 24 h (Fig 19) culture with Ni-Ti wires or control rods thymocytes were stained with propidium iodide and analysed by flow cytometry. Apoptotic cells were detected based on the smaller amount of genetic material, and thus the lower fluorescence intensity, as hypodiploid cells. Representative histograms are shown from one representative experiment.

After 24 h (Fig. 20) culture with Ni-Ti wires or control rods, thymocytes were stained with propidium iodide and



**Slika 21.** Učinek razmerja površina Ni-Ti-žic in prostornina medija, v odvisnosti od doziranja, na apoptozo timocitov v gojišču

**Figure 21.** Dose-dependent effect of Ni-Ti alloy's surface-to-volume of medium ratio on the apoptosis of thymocytes in culture

Po 24 h gojenja skupaj z Ni-Ti-žicami ali primerjalnimi paličicami so bili timociti obarvani s Turkovo raztopino in pregledani s svetlobno mikroskopijo. Apoptotične celice so bile ugotovljane s homogeno obarvanim heterokromatinom, medtem ko je bil delež apoptotičnih celic izračunan na osnovi analize vsaj 500 celic. Rezultati so prikazani kot srednja vrednost  $\pm$  SD ( $n = 5$ ) enega od reprezentativnih poskusov. \* $p < 0.05$ , \*\*\* $p < 0.005$ , v primerjavi z ustreznimi primerjalnimi vzorci (primerjalne steklene paličice).

## 6 Sklepi

Prispevek predstavlja funkcionalne lastnosti zlitin NiTi, zaradi katerih se uporabljajo v ortodontski praksi. Iz poznavanja mehanskih lastnosti ortodontskih žic lahko predvidimo, katera vrsta žic bo povzročala večje oziroma manjše sile na zobe med ortodontskim zdravljenjem. Mehanske lastnosti žic so v veliki meri odvisne od procesa izdelave, ki je zapleten in sestavljen iz velikega

analysed by flow cytometry. Apoptotic cells were detected based on the smaller amount of genetic material, and thus lower fluorescence intensity, as hypodiploid cells. Result are presented as mean  $\pm$  SD of three experiments \*\* $p < 0.01$ , \*\*\* $p < 0.005$ , compared to corresponding control samples (control glass rods).

In another experiment we investigated a dose-dependent effect of Ni-Ti orthodontic wires on the apoptosis of rat thymocytes in culture. The results are shown in Figure 21. It was shown that, within the surface-to-volume ratio of biomaterial in a medium that is recommended by ISO Standards (0.5 - 6 cm<sup>2</sup>/ml), only the highest amount of Ni-Ti wires increased apoptosis of thymocytes, which was higher significantly compared to spontaneous apoptosis in culture. The amount of Ni-Ti wires that was higher than the recommended one (8.0 and 12.0c m<sup>2</sup>/ml), increased apoptosis additionally, but without significant dose-dependent effect.

After 24h-culture with Ni-Ti wires or control rods, thymocytes were stained using Turk solution and analysed by light microscopy. Apoptotic cells were detected on the basis of homogenously stained heterochromatin, whereas the percentage of apoptotic cells was calculated by analysing at least 500 cells. The results are shown as mean  $\pm$  SD ( $n = 5$ ) from one representative experiment. \* $p < 0.05$ , \*\*\* $p < 0.005$ , compared to corresponding control samples (control glass rods).

## 6. Conclusions

The paper presents the essential features which make NiTi alloy used in orthodontic practice. By mechanical tests on orthodontic wires it is possible to predict which wire will cause a greater or lesser force on the tooth during orthodontic treatment.

števila različnih operacij. Pri tem obstajajo omejitve, ki so vezane na fazo hladnega preoblikovanja. Seveda pa je pri celovitem obravnavanju ortodontskih žic potrebno poznati tudi biološke vplive žic na človeško telo, saj so ti lahko škodljivi. Pri tem si lahko pomagamo s preskusi biokompatibilnosti. Zaradi posebnih lastnosti NiTi zlitine se te uporabljo na različnih področjih (medicina, letalstvo, vesoljska tehnologija, rekreacija). V prihodnosti pričakujemo uporabo teh zlitin na novih področjih, saj kot je predstavljeno v članku, lahko dosežemo različne mehanske lastnosti kljub omejitvam pri izdelavi (hladno oblikovanje).

Po drugi strani so preskusi biokompatibilnosti pokazali, da imajo vzorci Ni-Ti ortodontskih žic šibek citotoksičen učinek (indukcija apoptoze) na podganje timocite v gojišču, in to le za primer, ko je bilo uporabljeno največje razmerje površine zlitine in prostornine medija ( $6 \text{ cm}^2/\text{ml}$ ), ki je priporočeno z ISO standardom za preskušanje biokompatibilnosti.

However, it is important to know which wire has adverse effects on the human body, so it is necessary to perform a biocompatibility test. The mechanical properties of single wires have a significant impact on the production process of wires. It is a very complex process that requires a lot of different operations. Due to their specific characteristics SMA NiTi are already used in many different applications (medicine, aviation, space technology, recreation). However, it can be expected in the future in many new applications of these alloys because, as we present, the article may achieve different mechanical properties, although there are limits to the actual manufacture of these alloys (cold forming).

On the other hand, testing of biocompatibility presents that samples of Ni-Ti wires showed mild cytotoxic effect (induction of apoptosis) on rat thymocytes in culture, only when applied with the highest surface-to-volume ratio of alloy in medium ( $6 \text{ cm}^2/\text{ml}$ ) that is recommended by ISO Standards for biocompatibility testing.

## 7 Viri / References

- [1] H.G. Sergl: Festitzende Apparaturen in der Kieferorthopädie, Carl Hanser Verlag, München Wien, (1990).
- [2] K. Reitan, P. Rygh, Biomechanical principles and reactions, in T.M. Graber, R.L. Vanarsdall (eds.), Orthodontics: Current principles and techniques, St. Louis: Mosby, pp. 96-192, (1994).
- [3] J. Ferčec, B. Glišić, I. Šćepan, E. Marković, D. Stamenković, I. Anžel, J. Flašker, R. Rudolf, Determination of Stresses and Forces on the Orthodontic System by Using Numerical Simulation of the Finite Elements Method, A. Phys. Polonica A, vol. 122, pp. 659-665, (2012).
- [4] R.C. Scheid: Woelfel's Dental Anatomy: It's Relevance to Dentistry, 8th ed, Lippincott Williams&Wilkins, Philadelphia, PA, (2012).
- [5] S.A. Thompson, An overview of nickel-titanium alloys used in dentistry, Int. Endod. J., vol. 33, pp. 297-310, (2000).
- [6] D.C. Lagoudas, Shape Memory Alloy: Modelling and Engineering Applications, Springer, Texas (USA), (2008).
- [7] M.H. Wu, Fabrication Of Nitinol Materials and Components, SMST-SMM 2001, Kunming, China, pp. 285, (2001).

- [8] X.M. Wang, Z.F. Yue, Materials Science and Engineering, vol. 425, pp. 83-93, (2006).
- [9] Y. Liu, H. Yang, Materials Science and Engineering, vol. 260, pp. 240-245, (1999).
- [10] P.R. Kusy, A review of contemporary archwires: Their properties and characteristics, Angle. Orthod., vol. 67, pp. 197-207, (1997).
- [11] R. Rudolf, J. Ferčec, Force Measurement on Teeth Using Fixed Orthodontic Systems. Military Technical Courier, vol. 61(2), pp. 105-122, (2013). [12] M. Arndt, A. Bruck, T. Scully, A. Jager, C. Bourauel, Nickel ion release from orthodontic NiTi wires under simulation of realistic in-situ conditions, Journal of Materials Science, vol. 40(14), pp. 3659-3667, (2005).
- [12] M. Arndt, A. Bruck, T. Scully, A. Jager, C. Bourauel, Nickel ion release from orthodontic NiTi wires under simulation of realistic in-situ conditions, Journal of Materials Science, vol. 40(14), pp. 3659-3667, (2005).
- [13] T.H. Leea, T.K. Huangb, S.Y. Linc, L.K. Chend, M.Y. Choue, H.H. Huangf, Corrosion Resistance of Different Nickel-Titanium Archwires in Acidic Fluoride-containing Artificial Saliva, The Angle Orthodontist, vol. 80(3), pp. 547-553, (2010).

S. Müller, H. Pries, K. Dilger

Inštitut za spajanje in varjenje, Braunschweigova tehnološka univerza, Braunschweig, Nemčija /  
Institute of Joining and Welding, Braunschweig University of Technology, Braunschweig, Germany

## Izboljšanje procesa načrtovanja hladilnih sistemov pri kokilah za tlačno litje - občuten prispevek h kakovosti in življenjski dobi

### Enhancing the Design Process of Cooling Systems for Die-Casting Dies - A Significant Contribution to Quality and Lifetime

#### Izvleček

Pri visokotlačnem kokilnem litju nastopajo velike ciklične temperaturne in mehanske obremenitve. Cikli segrevanja in ohlajanja povzročajo toplotne raztezke in skrčke materiala, ustvarjajo napetostna polja, kar vodi do občutne plastične deformacije. Kopiranje plastičnih deformacij pogosto pripelje do nepričakovanih poškodb površine kokil za tlačno litje. Izbera, kakovost in obdelava (npr. toplotna obdelava) orodnih jekel za vroče preoblikovanje so parametri, o katerih se razpravlja v znanstveni literaturi. Vendar je krmiljenje temperature kokil za tlačno litje dodaten pomemben parameter, da se doseže primerna življenjska doba. Prispevek osvetljuje, kako se lahko značilne lastnosti klasičnih notranjih hladilnih sistemov (npr. koeficient prestopa toplote na steno in zmanjšanje tlaka) izračunajo s CFD-simulacijo (CFD – computational fluid dynamics – računalniška dinamika fluidov, op. prevajalca) (ANSYS CFX) in preverijo eksperimentalno. Izračunane specifične vrednosti zmanjšanja tlaka in koeficiente za prenos toplote na steno so bile obdelane in uporabljene za tehnične specifikacije. S tem znanjem je proces načrtovanja hladilnega sistema natančnejši kot pri ocenjevanju, ki sloni na dobljenih praktičnih izkušnjah. Vendar smo zaradi omejitve pri delovanju klasičnih hladilnih sistemov razpravljali o alternativni metodi, kako določiti usklajene hladilne kanale: razdelitev tlačne kokile na segmente. Da bi prikazali možnosti, prednosti in omejitve te metode, smo uporabili vložek iz obstoječe tlačne kokile. Prispevek se konča s kratkim povzetkom in pregledom pristopov za nadaljnje izboljšave.

**Ključne besede:** tlačno litje, proces načrtovanja, krmiljenje temperature, CFD-analiza, usklajeni hladilni kanali

#### Abstract

High-pressure die-casting dies are subjected to high cyclic temperatures and mechanical loads. Heating and cooling cycles cause thermal expansion and contraction of the material, generating strain fields which lead to a significant plastic deformation. An accumulation of plastic deformations often leads to unexpected failures at the surface of the die-casting die. The selection, quality and the processing (e. g. heat treatment) of hot work tool steels are parameters that are often discussed in scientific literature. However, the temperature control of the die-casting die is another important parameter for the achievement of reasonable lifetimes. The article illustrates, how characteristic properties of conventional internal cooling systems (e. g. the wall heat transfer coefficient and the pressure drop) can be calculated by CFD simulation (ANSYS CFX) and verified

by experimental investigations. The calculated specific values for the pressure drop and the wall heat transfer coefficient were processed and transformed into engineering specifications. Using this knowledge, the design process of the cooling system is more accurate than an estimated guess based on gained practical experience. However, due to restrictions in the performance of conventional cooling systems, an alternative method to establish conformal cooling channels is discussed: the segmentation of the die-casting tool. In order to demonstrate the potential, advantages and restrictions of this method, an existing die-casting tool insert is used. The article finishes with a brief summary and an outlook on further improvements to the approaches.

**Keywords:** die-casting, design process, temperature control, CFD analysis, conformal cooling channels

## 1 Uvod

Notranji hladilni sistem v kokili za tlačno ulivanje aluminija je namenjen predvsem za ustvarjanje toplotne bilance na določeni temperaturni ravni. [MEN99] je ugotovil, da je stroškovna učinkovitost proizvodnega procesa v veliki meri odvisna od dejstva, ali je orodje za litje učinkovit toplotni menjalnik. Ta trditev se je prvotno nanašala na vbrizgovalno ulivanje polimerov. Vendar so naraščajoči stroški dela, stroški energije in zahteve po kakovosti upravičili, da se ta trditev lahko uporabi tudi za tlačno litje. V osnovi ima hladilni sistem v kokili za tlačno litje vpliv na naslednje tri glavne vidike tlačnega litja:

- **čas cikla pri tlačnem litju:** učinkovit hladilni sistem omogoča, da se iz kokile za tlačno litje odstrani velika količina toplotne. Rezultat tega je skrajšan čas strjevanja, kar predstavlja dodatno skrajšanje časa cikla;
- **kakovost tlačno ulitih delov:** krmiljenje temperature in s tem krmiljeno strjevanje tlačno ulitega dela zmanjšuje na minimum tveganja za krčilne napake, ki se pojavi, kadar ni na razpolago materiala za napajanje, da kompenzira krčenje, ko se kovina struje. Učinkovit hladilni sistem ima vlogo, da pospeši ohlajanje nestrijenih

## 1 Introduction

The internal cooling system of an aluminum die-casting die primarily serves to establish a heat balance at a defined temperature level. [MEN99] stated that the cost effectiveness of the production process strongly relates to the question of whether the casting tool is an efficient heat exchanger. This statement was related to the injection moulding process originally. However, increasing labour costs, energy costs and demanding requirements in terms of quality justify the fact that this statement can also be seen in the context of the die-casting process. Basically, the cooling system of a die-casting die has an impact on the following three major aspects of the die-casting process.

- **The cycle time of the die-casting process:** An efficient cooling system enables the die-casting die to remove a high amount of heat. This results in a shortened solidification time which in turn implies a reduction of the cycle time.
- **The quality of the die-casting parts:** A temperature control and thus a controlled solidification of the die-casting part enable the minimization of the risk of shrinkage defects that occur when feed metal is not available to compensate

območij. Alternativno se lahko uporabi tudi za segretje lokalnih območij, da bi se zagotovil material za napajanje pri upočasnitvi strjevanja;

- **življenska doba tlačno ulitega materiala:** predhodne raziskave so navadno osredotočene na kakovost orodnega jekla za vroče preoblikovanje. V tem oziru sta metalurška sestava in obdelava (tj. tehnologije obdelave staljene kovine, topotna obdelava, razvoj površinskih prevlek) orodja za vroče preoblikovanje glavna kriterija. Cilj je ustvariti visokokakovostne materiale, da bi se povečala življenska doba tlačno ulitega materiala. Zato je velika ciklična obremenitev zaradi topotnih šokov neizogibno dejstvo. Glavna prednost učinkovitega hladilnega sistema je doseči zmanjšanje temperaturne razlike (in s tem zmanjšanje nateznih napetosti, ki jih povzroča topota) med kokilo za tlačno litje in mazivom kokile na vodni osnovi na minimum.

Vsota vseh teh vidikov kaže, da se hladilni sistem lahko obravnava kot bistveni parameter pri zagotavljanju gospodarnosti tlačnega litja. Kljub temu obstaja več težav, ki jih je treba razčistiti. Dimenzioniranje hladilnega sistema često sloni na pridobljenih izkušnjah konstruktorja kokile in tu manjka sistematični postopek načrtovanja [LIN03],[LI05]. Navadno imajo kokile za tlačno litje omejeno odvajanje toplotne in omejene topotne izgube zaradi neusklajenih hladilnih kanalov z omejenimi površinami ter slabo možnostjo krmiljenja temperature kokile. Dodatno so se v zadnjem času razvile in vpeljale tehnologije, pri katerih se uporablja minimalna količina pršil [MUE 12]. Čeprav ima ta metoda pršenja zanemarljiv vpliv na topotno bilanco kokile, obstajajo nadaljnji izzivi za razvoj notranjih hladilnih sistemov.

for shrinkage as the metal solidifies. An efficient cooling system possesses the function of an increased cooling of non-solidified areas. As an alternative, it serves to heat local areas in order to assure the feeding of material by decelerating the solidification process.

- **The lifetime of the die-casting material:** Preliminary research work commonly focused on the quality of the hot work tool steel. In this context, the metallurgical composition and the processing (e. g. molten metal processing technologies, heat treatment, development of surface coatings) of the hot work tool was regarded as a major criterion. The aim was to establish high-quality materials in order to strengthen the lifetime of the die-casting material. Consequently, the high cyclic loading due to thermal shocks was seen as an inevitable factor. The main advantage of an efficient cooling system is found in the minimization of the temperature difference (and thus in a reduction of thermally induced tensile strains) between the die-casting die and a water-based die lubricant.

The sum of all aspects indicates that the cooling system can be regarded as an essential parameter for ensuring an economic die-casting process. Nevertheless, there are several problematic issues that can be identified. The dimensioning of the cooling system is often based on the gained experience of the die-designer and lacks a systematic design process [LIN03], [LI05]. Usually die-casting dies exhibit a limited heat output and heat losses due to non-conformal cooling channels with limited surfaces and a poor controllability of the die temperature. In addition, the application of minimum quantity spraying technologies were developed and qualified recently [MUE12]. Since this spraying method has

Da bi spoznali preje omenjene izzive, je bil na Inštitutu za spajanje in varjenje pripravljen raziskovalni projekt. Strategija rešitve raziskovalnega projekta se je razdelila na dva pristopa: optimiranje z bolj učinkovitim dimenzioniranjem hladilnih kanalov in razdelitev kokile na segmente, da bi prišli do usklajenih hladilnih kanalov.

## 2 Osnove

### 2.1 Prenos toplote

Podrobne podatke o prenosu toplote med fluidom in trdnino lahko najdemo v številnih virih [BAE 12], [VDI06]. Da bi se osredotočili na glavno težavo, bomo v tem delu obravnavali vpliv osnovnih parametrov v enodimensijskem modelu prenosa toplote. S tem bomo prikazali, kako optimirati prenos toplote in njegove učinke. Gostoto toplotnega toka v trdnini zaradi prevajanja toplote lahko opišemo z enačbo 2-1 [BAE12]. Temu ustrezno enačba 2-2 opisuje gostoto toplotnega toka zaradi konvekcije fluida [BAE12]. Oba člena se lahko po pravilu o ohranitvi energije izenačita. Tako se lahko neznana temperatura stene ( $T_{wall}$ ) izloči, s čemer smo izpeljali enačbo 2-3. Oznake spremenljivk v enačbah 2-1 do 2-3 prikazuje slika 2-1. Enačba 2-3 je dobra osnova za razpravo o parametrih, ki imajo vpliv na toplotni tok. Tako slika 2-2 a-d ilustrira spremenjanje parametrov. Vsak diagram kaže spremenjanje ene spremenljivke; druge spremenljivke so pri tem konstantne.

Vidi se, da linearno povečanje toplotne prevodnosti povzroči eksponentno povečanje toplotnega toka. Orodna jekla za vroče preoblikovanje (npr. H11 ali H13) imajo navadno majhno toplotno prevodnost, kot prikazano na sliki 2-2a. Povečanje toplotne prevodnosti na vrednost 100 W/m.K občutno poveča toplotni tok.

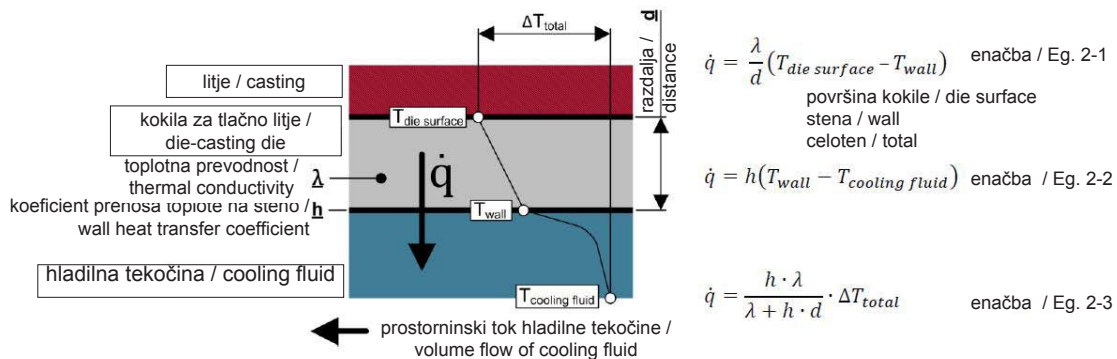
a negligible impact on the heat balance of the die, further challenges exist for the development of internal cooling systems.

In order to face the challenges mentioned above, a research project was conducted at the Institute of Joining and Welding. The solution strategy of the research project was split into two approaches: the optimization by a more efficient dimensioning of the cooling channels and the segmentation of the die in order to achieve conformal cooling channels.

## 2 Basics

### 2.1 Heat Transfer

Detailed information about the heat transfer between fluid and solid can be found in numerous sources [BAE12], [VDI06]. In order to focus on the main problem, only the influence of the basic parameters on a one-dimensional heat transfer model shall be considered in this section. This shall serve to point out the targets for a heat transfer optimization and its effects. The heat flux density in a solid due to heat conduction can be described according to equation 2-1 [BAE12]. Accordingly, equation 2-2 describes the heat flux density due to fluid convection [BAE12]. Both terms can be equated, based on the rule of energy conservation. Thus, the unknown wall temperature ( $T_{wall}$ ) can be eliminated and equation 2-3 is derived. The designation of the variables for the equations 2-1 to 2-3 can be obtained from Figure 2-1. Hence, equation 2-3 is a good base for a discussion of the parameters that have an influence on the heat flux. For that purpose, Figure 2-2 a-d illustrates the variation of parameters. Each graph depicts the variation of one variable; the other variables were set constant.



Slika 2-1. Shematični prikaz enodimensijskega sistema toplotnega toka

Figure 2-1. Schematic description of a one-dimensional heat flux system

Vendar se učinek zmanjšuje z večjimi vrednostmi toplotne prevodnosti. V osnovi je toplotna prevodnost jekel za vroče preoblikovanje omejena iz metallurških vidikov. Če razdelimo kokilo za tlačno litje na segmente, je razumno uporabiti materiale z boljšo toplotno prevodnostjo. Vpliv koeficiente prenosa topline na steno (slika 2-2b) kaže enako obnašanje kot toplotna prevodnost. Poleg tega se lahko ugotovi še dodatno pomembno dejstvo. Če pogledamo obliko krivulje, postane očitno, da mora biti glavni poudarek pri procesu načrtovanja na povprečnih vrednostih toplotnega prenosa.

Nadaljnja optimiranja, kar se tiče prenosa topline, bodo tudi povečala toplotni tok, vendar se bo njegov učinek občutno zmanjšal. Poleg tega se velike vrednosti koeficiente prenosa topline na steno lahko dosežejo samo z velikimi hitrostmi toka. Vpliv temperaturne razlike se lahko ugotovi iz slike 2-2c. Kot se vidi, povzroča naraščajoče spremenjanje temperature ustrezno konstantno spremenjanja toplotnega toka. Zato je ustreznije, da uporabljamo nizke temperature hladilnega sredstva. Poleg tega višja temperatura tudi povzroča večja napetostna nihanaj na površini. Glede na želeno daljšo življenjsko dobo materiala za

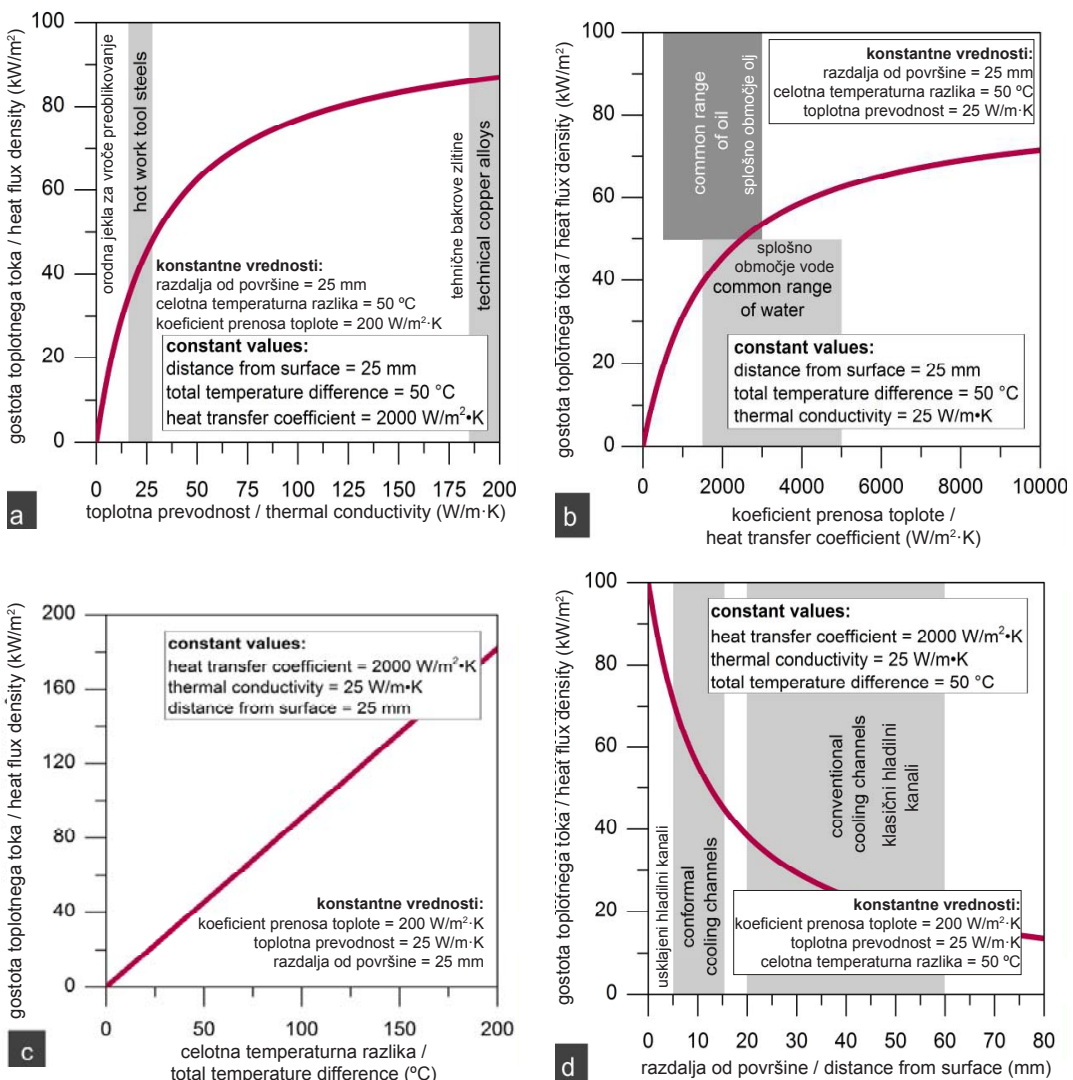
It becomes obvious that the effect of a linear increasing thermal conductivity results in an exponential increase of the heat flux. Hot work tool steels (e.g. H11 or H13) usually only possess a poor thermal conductivity as illustrated in Figure 2-2a. An increase of the thermal conductivity to a value of 100 W/m·K would enhance the heat flux significantly.

However, the impact decreases with higher values for the thermal conductivity. Basically, the thermal conductivity of hot work tool steels is restricted, due to metallurgical aspects. Nevertheless, in terms of the segmentation of a die-casting die, it is reasonable to use materials with a high thermal conductivity. The influence of the wall heat transfer coefficient (Figure 2-2b) exhibits an identical behaviour, compared to the thermal conductivity. In addition, further important information can be derived here. When examining the development of the graph, it becomes obvious that the main focus for the design process should be on ensuring the common values for the heat transfer.

Further optimizations regarding the heat transfer will also result in an increase of the heat flux, but the significance is substantially reduced. In addition to this

tlačno litje se je treba temu na vsak način izogniti in zato ta parameter ni uporaben za optimiranje. Zadnji parameter, ki ga prikazuje slika 2-2d, je razdalja od površine kokile. Jasno se vidi, da zmanjšanje razdalje vodi do občutno večjega topotnega toka zaradi eksponentne odvisnosti. To jasno potrjuje učinkovitost in uporabo

fact, high values for the wall heat transfer coefficient can only be obtained by very high values for the flow velocity. Information about the influence of the temperature difference can be derived from Figure 2.2c. As illustrated, increasing temperature changes lead to a corresponding constant change of the heat flux. Consequently, it is



Slika 2-2. Spreminjanje parametrov glede na enačbo 2-3

Figure 2-2: Variation of parameters according to equation 2-3

uskajenih hladilnih kanalov. Optimizacija tega parametra je omejena le z življenjsko dobo kokile, omejitvami pri konstruiranju (npr. pomanjkanje prostora) in posebnimi težavami, povezanimi z izdelavo.

Upoštevati je potrebno, da površina za menjavo toplote v tem primeru ni ovrednotena, ker delamo samo z enodimensijskim modelom. Pri dvo- ali tridimensijskih modelih je vpliv odvisen od velikosti in geometrije površin. Podatke o tem vplivu lahko najdemo v virih [BAE12], [VDI06]. Navadno povzroča večanje površin za menjavo toplote občutno večje toplotne tokove.

## 2.2 Zmanjšanje tlaka

Poglavje 2-1 je odkrilo, da je zelo pomembno ustvariti ustrezen hitrost toka v hladilnih kanalih, da bi se zagotovil dovolj velik koeficient prenosa toplote na steno. Vendar je tok skozi hladilne kanale povezan z zmanjšanjem tlaka. To zmanjšanje tlaka je posledica trenja ob stenah in trenjskih sil v hladilnem sredstvu [SIG12]. Slika 2-3 ilustrira to težavo za preprost sistem hladilnih kanalov v vložku kokile za tlačno litje. Enačbi 2-4 in 2-5 slonita na Bernouillijevi enačbi, z njima pa se zmanjšanje tlaka opisuje analitično [SIG12]. Da bi se dobilo preprosto rešitev, smo uporabili več predpostavk. Kot se lahko izpelje iz enačbe 2-6, se celotno zmanjšanje tlaka lahko razdeli na tri posamezne dele [NOG10].

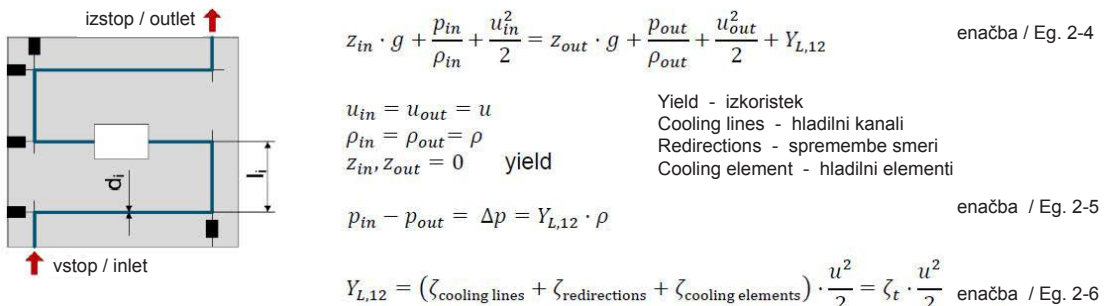
Enačba 2-7 opisuje, da je celotni koeficient trenja hladilnega sistema posledica treh delnih zmanjšanj tlaka [NOG10]. Celoten koeficient trenja je tudi posledica dveh mehanizmov: člen 1 opisuje vpliv koeficiente trenja ob steni; člen 2 opisuje koeficient trenja kot posledico ovir (npr. sprememba smeri ali hladilni elementi) v območju toka. Primer je prikazan na sliki 2-3, kjer celoten koeficient trenja določa

eligible to operate with low temperatures of the cooling fluid. However, a higher temperature difference also leads to larger stress amplitudes at the die surface. With respect to a high lifetime of the die-casting material, this should be avoided by all means and therefore this parameter is not applicable for the optimization. The last parameter illustrated in Figure 2-2d is the distance from the die surface. As it can be seen clearly, a decrease of the distance leads to a substantial higher heat flux due to an exponential correlation. This clearly substantiates the effectiveness and application of conformal cooling channels. The optimization of this parameter is limited only by restrictions due to the lifetime of the die, design restrictions (e. g. a lack of space) and especially problems associated with production.

Note that the area of the heat exchanging surface is not evaluated in this example since this is only a one-dimensional model. For two or three-dimensional models, the influence depends on the surface area and the geometry of the surfaces. Information about this influence can be found in the literature [BAE12], [VDI06]. Usually, an increase of heat exchanging surfaces also leads to a significantly higher heat flow.

## 2.2 Pressure Drop

Chapter 2.1 revealed that it is essential to establish an adequate flow velocity in the cooling channels in order to ensure a sufficient wall heat transfer coefficient. However, a pressure drop results from the flow through the cooling channels. This pressure drop originates from the wall friction and frictional forces within the cooling fluid [SIG12]. Figure 2-3 shall serve to illustrate this issue for a simple cooling channel system in a die-casting die insert. The equations 2.4 and 2.5 are based on Bernoulli's principle and are used to



Slika 2-3. Shematičen prikaz toka fluida in različnih odporov toku

Figure 2-3. Schematic description of a one-dimensional heat flux system

specifična površina hladilnega sistema, premer izvrtine, podatek o hrapavosti površine in specifični koeficient trenja za en hladilni element ter šest sprememb smeri.

$$\zeta_t = \lambda_i \cdot \frac{l_i}{d_i} + \sum_{k=1}^n \zeta \cdot \frac{A_{ind}^2}{A_{ref}^2} \quad \text{enačba / Eg. 2-7}$$

člen 1 / term 1 člen 2 / term 2

kjer je

$\lambda_i$	koeficient trenja ob steni
$l_i$	skupna dolžina hladilnega kanala
$d_i$	premer izvrtine
$A_{ref}$	primerjalni prerez za izračun koeficienteva trenja
$A_{ind}$	posamezni primerjalni prerez hladilnega elementa

Narejene so bile obsežne raziskave, da bi se lahko opisal koeficient trenja ob steni, podatki pa se lahko najdejo v literaturi [LAU09], [SIG12]. Enako velja za spremembe smeri toka v kokili za tlačno litje [NOG10], [MEN99], [VDI06], čeprav preiskane geometrije često komaj ustrezajo geometriji v kokili za tlačno litje (geometrija, ki je posledica križanja dveh izvrtin). Glavni poudarek bo dan hladilnim elementom, ker ti elementi navadno povzročajo največje zmanjšanje tlaka in zato zahtevajo natančno ovrednotenje. Vrednost koeficienteva trenja

describe the pressure drop analytically [SIG12]. In order to retrieve a straightforward solution, several assumptions were made. As it can be derived from equation 2.6, the pressure drop is divided into three individual losses [NOG10].

Equation 2-7 describes the total friction factor of the cooling system that originates from the three losses [NOG10]. The total friction factor results from two different mechanisms: Term 1 describes the influence of the wall friction factor; Term 2 describes a friction factor that originates from obstacles (e. g. redirections or cooling elements) in the flow passage region. For the example given in Figure 2-3, the total friction factor is determined by a specific length of the cooling system, the diameter of the bore, information about the surface roughness and by a specific friction factor for one cooling element and six redirections.

$\lambda_i$	wall friction factor
$l_i$	accumulated length of the cooling channel
$d_i$	bore diameter
$A_{ref}$	reference cross section of the calculated friction factor
$A_{ind}$	individual reference cross section of the cooling element

Extensive research has been conducted in order to describe the wall friction so

za hladilni element mora biti odvisna od hitrosti toka. Ker hitrost toka v hladilnem elementu ni konstantna zaradi različnim prerezov, prevez primerjalnega premora nudi enak odpor kot celoten sistem odporov (v našem primeru Aind). Enačba 2-8, ki sledi, opisuje izračun koeficiente trenja in izkoristke iz preje omenjenih enačb 2-5 in 2-6. Ta enačba se uporablja, da pretvori rezultate izračuna zmanjšanja tlaka, ki smo jih dobili s preskusi in numeričnimi izračuni, v koeficient trenja. Ker hitrost toka znotraj hladilnega elementa ni konstantna, se uporabi primerjalna hitrost (ki se dobi na osnovi primerjalnega prereza). Ustrezna vrednost tega prereza bi bil prevez ostalih hladilnih kanalov, ki so izdelani z orodjem za globoko vrtanje izvrtin.

$$\zeta = \frac{\Delta p}{\frac{\rho}{2} \cdot u^2}$$

enačba / Eg. 2-8

kjer je

$\Delta p$	tlačna razlika med vstopom in izstopom
$\rho$	gostota fluida za hlajenje/prenos toplote
$u$	hitrost fluida za hlajenje/prenos toplote

### 3 CFD-izračun parametrov hladilnega sistema

Da bi dobili ustrezno zanesljive parametre, je bilo treba upoštevati naslednje pomembne vidike [ANS10b]:

- podrobno modeliranje geometrije hladilnega kanala,
- skrbna izbira modela fluida (npr. turbulentnega modela),
- združitev primernih lastnosti materiala in
- izbira ustreznih robnih pogojev.

Za analizo je bila uporabljena računalniška oprema ANSYS CFX. Prvi

that further information can be found in the literature [LAU09], [SIG12]. The same applies to the redirections in the die-casting die [NOG10] [MEN99] [VDI06], although the examined geometries often hardly correspond to the geometry that exists in the die-casting die (a geometry that results from the crossing of two bores). The main emphasis shall be put on the cooling elements since the elements usually induce the highest pressure drop and hence require a precise evaluation. The value of the friction factor for the cooling element must be referred to a flow velocity. Since the flow velocity within the cooling element is not constant due to different profiles, the cross section of a reference diameter is integrated (here: Aind).

The equation 2.8 stated below describes the calculation of the friction factor and yields from the equations 2.5 and 2.6, mentioned above. This equation is used to transform the pressure drop results, derived from experimental and numerical investigations, to a friction factor. Since the flow velocity inside of the cooling element is not constant, a reference velocity (which results from a reference cross section) has to be used here. A reasonable value for this cross section would be the cross section of the remaining cooling channels that are manufactured by deep hole drilling tools.

$\Delta p$	pressure difference between inlet and outlet
$\rho$	outlet density of the cooling/ heat transfer fluid
$u$	fluid velocity of the cooling/ heat transfer fluid

### 3 CFD-BASED EVALUTION OF COOLING SYSTEM PARAMETERS

In order to retrieve reliable results, the following major aspects necessarily should be considered [ANS10b]:

- the detailed modeling of the cooling

korak je modeliranje geometrije hladilnega kanala. Ker to zahteva izračun prenosa topote na steno, sta bili modelirani dve območji: območje fluida (geometrija hladilnega kanala) in območje trdnine (kokila za tlačno litje). Materialne lastnosti materiala, odvisne od temperature, se lahko dobe za večino hladilnih tekočin in so bile integrirane v simulacijo. Ker se hladilne tekočine navadno uporabljajo v sorazmerno ozkem temperaturnem območju, so se za določene simulacije uporabile konstantne materialne vrednosti.

Večina preiskanih tokov je turbulentnih [SIG12], [NOG10]. Raje pa imamo za naš namen stacionarne simulacije, ker so krajše, naknadna obdelava je preprostejša, navadno pa nas zanimajo povprečne časovne vrednosti [EGG11]. Zato smo uporabili Reynolds-povprečni Navier-Stokesov model (RANS – Reynolds-Averaged Navier-Stokes (op.prevajalca)) in strižno-napetostni model prenosa (SST) kot turbulenčni model. Ta model združuje prednosti  $k-\varepsilon$  modela in  $k-\omega$  modela ter se lahko obravnava kot industrijski standard za modeliranje turbulence, ker so ga številne aplikacije verificirale, njegovo delovanje je robustno za večino mrežnih topologij, ima dobro interoperabilnost z drugimi fizikalnimi modeli in prefinjeno obravnava steno [EGG11]. Pri vseh izračunih smo uporabili robne pogoje brez zdrsa. Hitrost fluida je ob steni nič, kar je dober približek realnemu toku fluida. Da bi bil izračun koeficiente prenosa topote na steno zaupanja vreden, je bilo treba skrbno paziti na modeliranje mejnih plasti. Zato je bilo treba zagotoviti, da so bili hitrostni profil fluida in pojavi prenosa energije v območju sten pravilno modelirani [ANS10a], [ANS10b].

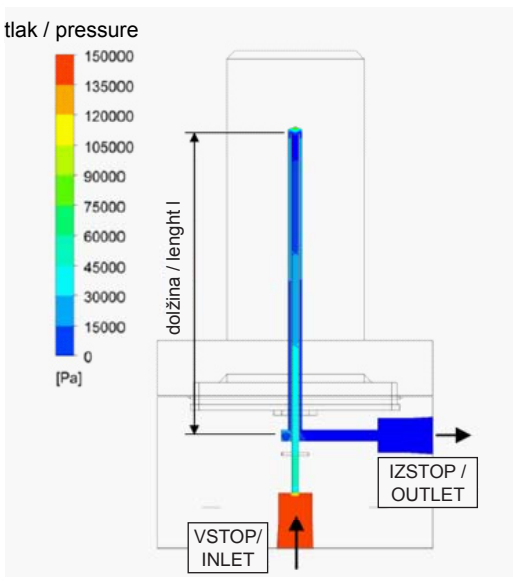
Slika 3-1 prikazuje tipični rezultat za zmanjšanje tlaka pri kaskadnem spoju vodnih kanalov s premerom izvrstice 5 mm. Kot robni pogoj je bilo postavljeno, da je

channel geometry,

- the careful selection of the fluid model (e.g. the turbulence model),
- the integration of suitable material properties and
- the selection of reasonable boundary conditions.

The analyses were carried out by the software ANSYS CFX. The first step is the modeling of the cooling channel geometry. Since it is required for the calculation of the wall heat transfer, two domains are modeled: the fluid domain (the cooling channel geometry) and the solid domain (the die-casting die). Temperature dependent material properties of the major cooling fluids are accessible and were integrated into the simulation. Since the cooling fluid is usually operated at a rather narrow temperature range, constant material properties were used for a specific simulation setup.

The majority of examined flows are turbulent [SIG12], [NOG10]. Steady state simulations are preferred for this application because they exhibit a shorter simulation time, post-processing is simplified and usually only time-averaged values are of interest [EGG11]. Hence, a Reynolds-Averaged Navier-Stokes model (RANS) is applied. Accordingly, the Shear-Stress-Transport model (SST) was selected as a turbulence model. This model combines the advantages of the  $k-\varepsilon$  and the  $k-\omega$  model and can be regarded as an industrial standard for turbulence modeling since it has been validated for a broad range of applications, shows a robust performance on most of the mesh topologies, has a good interoperability with other physical models and exhibits a sophisticated treatment of the wall [EGG11]. For all of the conducted calculations, a *no-slip* boundary condition was applied. The fluid will have zero velocity relative to the boundary which is a good

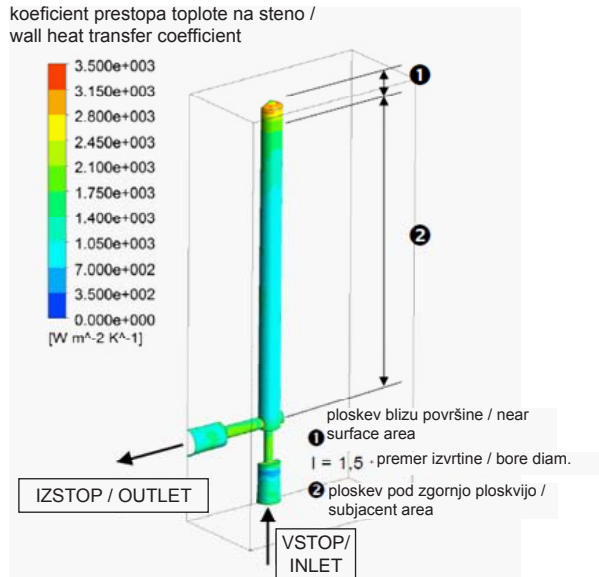


**Slika 3-1.** Zmanjšanje tlaka zaradi toka fluida pri kaskadnem spoju vodnih kanalov (hladilna tekočina: voda, povprečna temperatura: 50 °C, premer izvrtine: 5 mm, hitrost toka na vstopu: 2,5 l/min)

**Figure 3-1.** Pressure drop due to a fluid flow in a cascade water junction (cooling fluid: water, averaged temperature: 50 °C, bore diameter: 5 mm, flow velocity at the inlet: 2,5 l/min)

hitrost toka na vstopu konstantna in da ima tlak na izstopu vrednost atmosferskega tlaka (1 bar).

Razlika tlakov je bila izračunana iz razlike med tlakom na vstopu in tlakom na izstopu, v našem primeru pa je bila okoli 1,3 bar. Ker je za izračun potrebno le celotno zmanjšanje tlakov hladilnega elementa, ni pomembno vrednotenje lokalnih površin. Slika 3-2 prikazuje porazdelitev koeficiente prenosa toplote na steno. Zapomnimo si, da je prenos toplote funkcija Reynoldsovega števila in geometrije ter temperaturne razlike sistema ( $T_{stena}/T_{hladilni\ fluid}$ ). Zato ni uresničljivo ugotoviti samo eno vrednost za koeficient prenosa toplote na steno, ampak



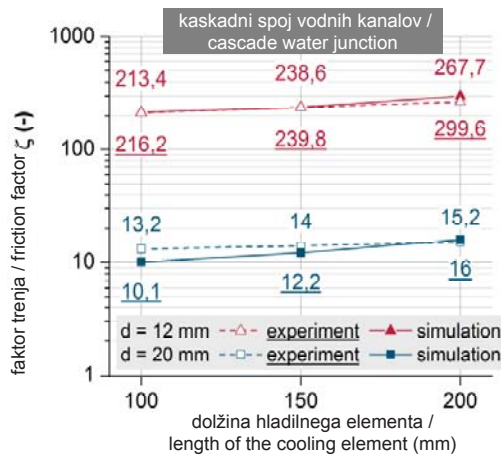
**Slika 3-2** Koeficient prenosa toplote na stene v ovisnosti od geometrije stene pri kaskadnem spoju vodnih kanalov (hladilna tekočina: voda, povprečna temperatura: 50 °C, premer izvrtine: 12 mm, hitrost toka na vstopu: 20,5 l/min)

**Figure 3-2.** Geometry dependent wall heat transfer coefficient of a cascade water junction (cooling fluid: water, inlet temperature: 50 °C, bore diameter: 12 mm, flow velocity at the inlet: 20,5 l/min)

approximation of the real fluid flow. In order to calculate a trustworthy wall heat transfer coefficient, the modeling of the boundary layers has to be carefully attended to. Thereby, it is ensured that the velocity profile of the fluid and the energy transport phenomena at the wall regions are modeled correctly [ANS10a], [ANS10b].

Figure 3-1 exemplarily shows the result for the pressure drop in a cascade water junction with a bore diameter of 5 mm. As a boundary condition, the flow velocity at the inlet was set to constant and pressure at the outlet was set to atmospheric pressure (1 bar).

primerjava faktorja trenja – eksperimentalni in računski rezultati /  
comparison of the friction factor – experimental and numerical results

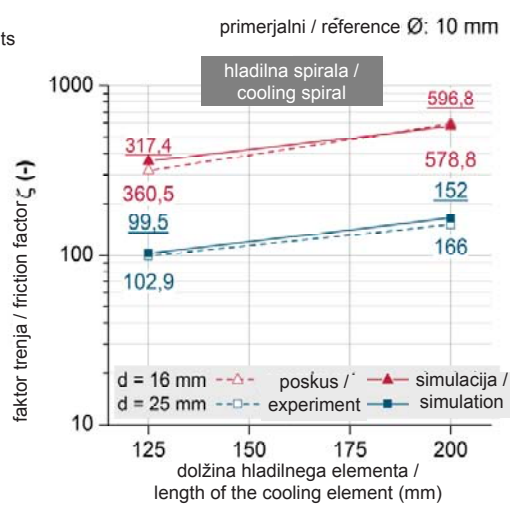


**Slika 3-3.** Primerjava faktorjev trenja za različne kaskadne spoje vodnih kanalov, ugotovljenih eksperimentalno in z CFD-simulacijami

**Figure 3-3.** Comparison of friction factors for various cascade water junctions, determined by experimental measurements and CFD simulations

Številsko rešitev za celotni hladilni element. Da bi se poenostavil vpliv geometrije, sta bili definirani dve območji: ploskev blizu površine (1) in ploskev tik pod njo (2). Potem so se ugotovile povprečne vrednosti koeficiente prenosa toplote na steno za vsako območje. Zaradi omejitev modela, prikazanih na sliki 3-2, so bili izračunani koeficienti prenosa toplote na steno med  $3000 \text{ W/m}^2 \text{ K}$  (blizu površine kokile) in  $1000 \text{ W/m}^2 \text{ K}$  (na spodaj ležečih ploskvah).

Rezultati izračunanih faktorjev trenja so bili eksperimentalno preverjeni. Zaradi industrijske pomembnosti so bili preiskani različni kaskadni spoji vodnih kanalov in hladilnih spiral. V tem kontekstu kažeta dobljene rezultate sliki 3-3 in 3-4. Iz obeh diagramov se vidi, da je odstopanje med izračunanimi in eksperimentalnimi rezultati zanemarljivo majhno glede na stopnjo natančnosti, ki je želena pri tehničnem



**Slika 3-4.** Primerjava faktorjev trenja za različne hladilne spirale, ugotovljenih eksperimentalno in z CFD-simulacijami

**Figure 3-4.** Comparison of friction factors for various cooling spirals, determined by experimental measurements and CFD simulations

The pressure difference is calculated from the pressure difference at the inlet and at the outlet, in this case the pressure drop is about 1.3 bar. Since only the total pressure drop of a cooling element is necessary for a calculation, the evaluation of local areas is not relevant. Figure 3-2 illustrates the distribution of the wall heat transfer coefficient. Note that the heat transfer is a function of the Reynolds number, the geometry and the temperature difference of the system ( $T_{\text{wall}}/T_{\text{cooling fluid}}$ ). Hence, it is not feasible to determine only one parameter for the wall heat transfer coefficient but a parametric solution for a cooling element. In order to simplify the influence of the geometry, two areas were defined: the near surface area (1) and the subjacent area (2). Afterwards, the results for the wall heat transfer coefficient were averaged for each area. For the

konstruiranju. V nadaljevanju ni bilo sistematičnih odstopanj. Ker je bila ta stopnja ujemanja dosežena pri različnih geometrijah in velikostih hladilnih elementov, predlagamo, da se metoda računanja lahko prenese tudi na druge hladilne geometrije.

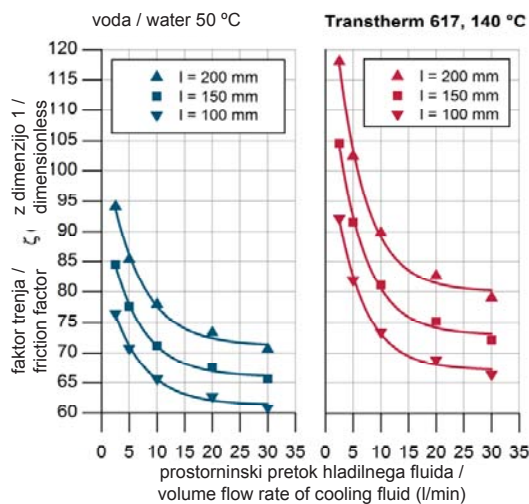
Poleg tega smo naredili poskuse, da bi preverili izračunane vrednosti koeficiente prenosa toplote na steno. V tem primeru so bile izračunane vrednosti tudi preverjene (ni prikazano tukaj). Vendor smo opazili majhno sistematično odstopanje med računskimi in eksperimentalnimi rezultati: izračunani koeficient prenosa toplote na steno je bil večji od izmerjene vrednosti za faktor 1,05 – 1,10. Vzrok za to se lahko najde v dejstvu, da numerična simulacija predpostavlja idealno steno brez onesnaženja na mejni površini. Kljub temu se lahko razume, da so izračunane vrednosti dovolj zanesljive glede na stopnjo natančnosti, ki je potrebna za tehnično konstruiranje, in se zato lahko uporabijo v procesu konstruiranja. Slika 3-5 kaže rezultate 30 izračunov za ugotavljanje faktorja trenja za kaskadne spoje vodnih kanalov različnih dolžin (prim. slika 3-1). Uporabljena enota na x-osi je bila l/min, ker se ta navadno uporablja v livarnah in pri enotah za krmiljenje temperature. Izpelje se lahko iz dejstva, da faktor trenja ni konstantna vrednost ampak funkcija pretoka hladilnega fluida. Uporablja se predvsem za majhne hitrosti tokov. Daljši kaskadni spoji vodnih kanalov povzročajo večja zmanjšanja tlaka. Zato imajo ti elementi večji faktor trenja. Računali smo z dvema vrstama fluidov: vodo z materialnimi lastnostmi fluida pri 50 °C in fluidom TRANSTHERM 617 za prenos toplote z materialnimi lastnostmi fluida pri 140 °C (prim. [MAR06] s primerljivimi lastnostmi fluida). Izbirali smo na osnovi dejstva, da je med obema fluidoma razmeroma velika razlika viskoznosti in zaradi tega imata različne faktorje trenja. Izbera več materialov bi bila prezapletena

model constraints described in Figure 3-2, wall heat transfer coefficients from 3000 W/(m<sup>2</sup>K) (at the near surface areas) and 1000 W/m<sup>2</sup>K (at the subjacent areas) were calculated.

The results for the calculated friction factor were validated by experimental investigations. Due to its industrial relevance, various water cascade junctions and cooling spirals were examined. In this context, Figures 3-3 and 3-4 display the achieved results. It can be taken from both diagrams that the deviation of the numeric results and the experimental results is negligible in respect of a degree of accuracy that is desirable for engineering design. Furthermore, there is no systematic deviation. Since this degree of accordance was achieved for various cooling element geometries and sizes, it was suggested that the calculation method can be transferred to further cooling geometries.

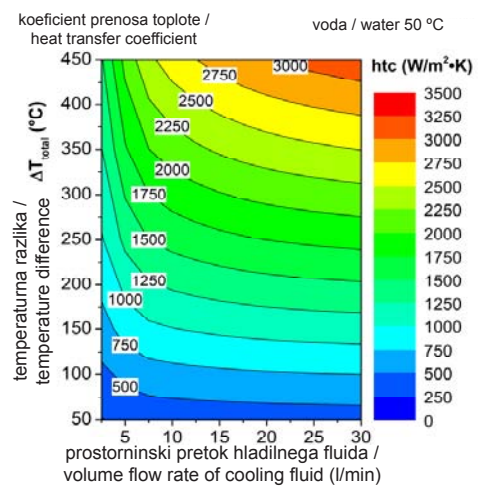
Moreover, experimental research was conducted in order to verify the calculated results for the wall heat transfer coefficient. In this case, the calculated results also were verified (not illustrated here). However, a slight systematic deviation was observed between the numeric and the experimental results: the calculated wall heat transfer coefficient exceeded the measured value by the factor 1,05 -1,10. The reason for this deviation can be found in the fact that the numeric simulation assumes an ideal wall without any contaminations at the boundary surface. Nevertheless, the calculated results for the wall heat transfer coefficient can be regarded as trustworthy in a respect of a degree of correctness that is worthwhile for engineering design and therefore can be used for the design process.

Figure 3-5 displays the results of 30 calculations for determining the friction factor of a cascade water junction with various lengths (c. f. Figure 3-1). The unit



**Slika 3-5.** Izračunani faktorji trena v odvisnosti od pretoka fluida pri kaskadnem spoju vodnih kanalov, primerjalni premer je 16 mm

**Figure 3-5.** Calculated friction factor due to fluid flow in a cascade water junction; reference diameter is 16 mm



HASCO kaskadna povezava vodnih kanalov / HASCO cascade water junction  
povprečno ovrednotenje spodaj ležeče ploskve / averaged evaluation of the subjacent area

**Slika 3-6.** Izračunani koeficienti prenosa topote na steno pri kaskadni povezavi vodnih kanalov (spodaj ležeče ploskve)

**Figure 3-6.** Calculated wall heat transfer coefficient in a cascade water junction (subjacent areas)

za obdelovanje, ker vsaka krivulja zahteva več računanj. Diagram na sliki 3-5 omogoča uporabniku z vidika celotnega zmanjšanja tlaka izbiro med dvema fluidoma. Voda pri 50 °C naj bi se izbrala, če se uporablja voda ali hladilni fluid na osnovi vode (v kateremkoli temperaturnem območju). Rezultati z TRANSTHERM 617 so uporabni, kadar se uporablja fluid za prenos topote pri razmeroma nizki temperaturi (100-160 °C).

Slika 3-6 kaže izračunane koeficiente prenosa topote na steno hladilnega elementa kot funkcijo temperaturne razlike in prostorninskega pretoka. Uporabili smo dvodimensijske interpolacije ter funkcijo za glajenje krivulje, da bi ponazorili rezultate numeričnih izračunov. Slika 3-6 velja za vodo kot hladilno sredstvo in se nanaša na spodnjo plast (prim. sliko 3-2). Tu je koeficient prenosa topote na

of the x-axis was set to " /m<sup>n</sup>" since its use is common in foundries and temperature control units. It can be derived from that the friction factor is not a constant value but a function of the cooling fluid flow rate. This especially applies for low values of the flow velocity. Longer water cascade junctions cause a higher pressure drop. Hence, these elements exhibit an increased friction factor. The calculations were done for two fluids: water with fluid material properties that correspond to a temperature of 50 °C and TRANSTHERM 617 heat transfer fluid with fluid material properties that correspond to a temperature of 140 °C (cf. [MAR06] with comparable fluid properties). The selection is founded on the fact that both fluids exhibit a relatively high difference in the viscosity and thus exhibit different friction factors. The selection of more materials would be too complex to handle since every graph needs

steno eksponentna funkcija pretoka (in s tem tudi Reynoldsovega števila). Vpliv prostorninskega pretoka je pomemben pri majhnih pretokih in se manjša, ko se povečuje pretok. Poleg tega spremišanje temperaturne razlike vodi do ustrezne konstantne spremembe koeficienta prenosa toplotne na steno (glede na sliko 2-2c). Na tej sliki je temperaturna razlika  $\Delta T_{\text{total}}$  izračunana iz povprečne temperature kokile (na oddaljeni točki, kjer ni neposrednega vpliva hladilnega elementa) in povprečne temperature hladilnega sredstva. Nadaljnji izračuni bodo dali vrednost na določeni razdalji od hladilnega elementa. S tem bo lahko uporabnik pri simulaciji litja (npr. MAGMASOFT) uporabil temperaturno odvisni koeficient za prenos toplotne na steno.

#### 4. Izvedba optimiranega hladilnega sistema

Dobljeni rezultati so nas opogumili, da uporabimo metode računanja za obstoječi kokilni vložek kokile za tlačno litje. Zato je bilo treba preiskati možnost optimiranja toplotnega toka za vso kokilo za tlačno litje. Uporabili smo dve metodi načrtovanja, da bi se povečal toplotni tok: optimalno mesto klasičnih hladilnih elementov in uporaba strategije delitve na segmente. Zato slike 4-1a do 4-1c predstavljajo konstrukcije hladilnih kanalov.

Slika 4-1a kaže začetno konstrukcijo hladilnih kanalov, izdelanih z globokim vrtanjem izvrtin. Po ovrednotenju te konstrukcije smo izračunali različne optimizacije. Končna konstrukcija optimizacije s klasičnimi hladilnimi elementi (vzporedna/serijska vezava obojnih elementov) je prikazana na sliki 4-1b. Nazadnje slika 4-1c prikazuje obrise uporabljenega segmenta. V tem primeru

several calculations. In terms of the total pressure drop, the diagram shown in Figure 3-5 enables the user to select between two fluids. Water 50 °C should be selected if water or water-based cooling fluid (at any temperature range) is used. The results of TRANSTHERM 617 are applicable if a heat transfer fluid is used with a comparatively low temperature (100-160 °C).

Figure 3-6 displays the calculated wall heat transfer coefficient of the cooling element as a function of the temperature difference and the volume flow rate. A two-dimensional interpolation and a smoothing function were used in order to illustrate the results of numerous calculations. The Figure 3-6 is valid for water as a cooling fluid and corresponds to the subjacent area (cf. Figure 3-2). Here, the wall heat transfer coefficient is an exponential function of the flow rate (and thus the Reynolds number). The influence of the volume flow rate is significant at low values of the flow rate and reduces with an increase of the flow rate. Moreover, a change in the temperature difference leads to a corresponding constant change of the wall heat transfer coefficient (according to Figure 2-2c). In this Figure, the temperature difference  $\Delta T_{\text{total}}$  originates from the average temperature of the die (at a remote point which is not influenced directly by the cooling element) and the average temperature of the cooling medium.

Further calculations will display the value for a defined distance from the cooling element. Thereby, the user is enabled to implement a temperature dependent wall heat transfer coefficient in the casting simulation (for instance MAGMASOFT).

#### 4 Implementation of an Optimized Cooling System

The achieved results encouraged to apply the calculation methods to an existing die-

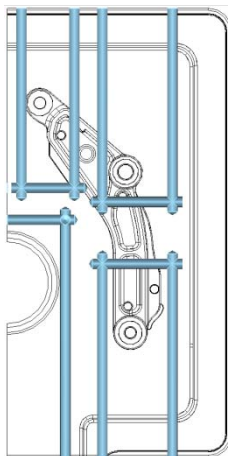
je območje hlajenja 7,5 mm pod površino livne votline, vstopna in izstopna odprtina sta integrirani v segment, zato nista vidni.

Slike 4-2a do 4-2c kažejo rezultate pretoka fluida in pojasnjujejo izboljšanje toplotnega izkoristka kokile za tlačno litje. V tem primeru je bila kokila za tlačno litje (materialne lastnosti so ustrezale orodnemu jeklu za vroče preoblikovanje H11) nastavljena na začetno temperaturo 400 °C. Temperatura hladilne vode je bila nastavljena na 50 °C in hitrost toka na 20 l/min. Po 60 s delovanja je bila izračunana srednja temperatura površine livne votline. Ta model bo uporabljen za ugotavljanje delovanja hladilnih sistemov pri odvajanju velike količine toplote.

casting die insert. Hence, the potential to optimize the heat flux of the whole die-casting die ought to be examined. Two design methods were used in order to increase the heat flux: the optimized allocation of conventional cooling elements and the application of segmentation strategies. For this reason, Figure 4-1a to Figure 4-1c display the design of the cooling channels.

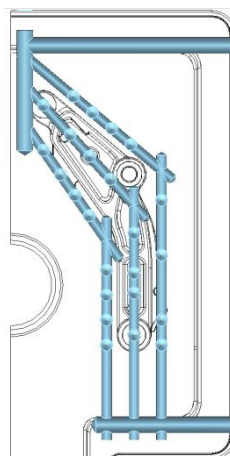
Figure 4-1a shows the initial design of the cooling channels, manufactured by deep hole drilling. After the assessment of this design, various optimizations were calculated. The final design of an optimization with conventional cooling elements (a parallel/series connection of baffle elements) is illustrated in Figure 4-1b. Finally, Figure 4-1c shows the contour of the applied die segment. In this case, the cooling area is located 7,5 mm beneath the surface of the cavity, the inlet and outlet is integrated into the segment, hence it is not visible here.

Figure 4-2a to Figure 4-2c display the results of a transient fluid simulation and clarify the enhancements in the thermal output of the die-casting die. Here, the die-casting die (material properties correspond to a H11 hot work tool steel) was set to an initial temperature of 400 °C. The temperature of the cooling fluid water was set to 50 °C and the flow



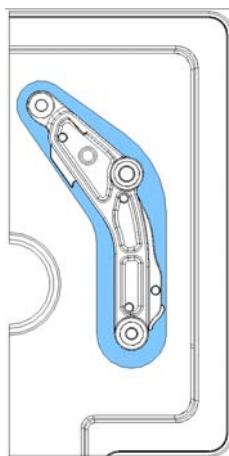
**Slika 4-1a.** Začetna konstrukcija hladilnih kanalov

**Figure 4-1a.** Initial design of the cooling channels



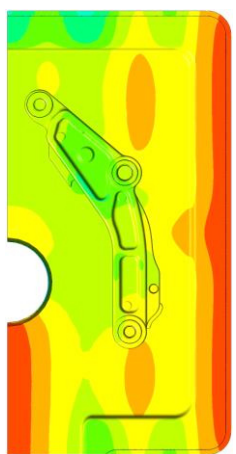
**Slika 4-1b.** Optimirana konstrukcija klasičnih hladilnih elementov

**Figure 4-1b.** Optimized design of conventional cooling elements



**Slika 4-1c.** Delitev kokilnega vložka na segmente, usklajeni hladilni kanali

**Figure 4-1c.** Segmentation of the die insert, conformal cooling channels



**Slika 4-2a.** Povprečna temperatura na površini livne votline kokile: 305 °C

**Figure 4-2a.** Average temperature at the cavity surface of the die: 305 °C



**Slika 4-2b.** Povprečna temperatura na površini livne votline kokile: 124 °C

**Figure 4-2b.** Average temperature at the cavity surface of the die: 124 °C



temperaturna porazdelitev po 60 s /  
temperature distribution after 60 s

**Slika 4-2c.** Povprečna temperatura na površini livne votline kokile: 69 °C

**Figure 4-2c.** Average temperature at the cavity surface of the die: 69 °C

## 5 Povzetek in sklepi

Prispevek opisuje glavne vplivne parametre za optimizacijo odvajanja toplote iz kokile za tlačno litje. Pokazano je bilo, da sta razdalja od površine livne votline in koeficient prenosa toplote na steno bistvena parametra, da se izboljša odvajanje toplote iz kokile za tlačno litje. Da se doseže zanesljive vrednosti koeficijenta za prenos toplote na steno, je potrebno poznati hitrost toka fluida za prenos toplote. Zato so bile opisane metode za računanje faktorja trenja hladilnih elementov s trgovsko CFD-računalniško opremo, imenovano ANSYS CFX. Izračunani rezultati so se primerjali z rezultati poskusov in ugotovljeno je bilo dobro ujemanje. Poleg tega je bila uporabljena metoda končnih elementov za modeliranje prenosa toplote med fluidom in odvajanje toplote in kokilo za tlačno litje.

velocity was set to 20 l/min. After a runtime of 60 s, the mean temperature at the cavity surface was evaluated. Hence, this model shall serve to determine the performance of the cooling systems in respect to a high heat output.

## 5 Summary and Concusions

The article described the major influencing parameters for a heat output optimization of the die-casting die. It was pointed out that the distance from the cavity surface and the wall heat transfer coefficient are essential parameters in order to increase the heat output of the die-casting die. In order to achieve reliable values for the wall heat transfer coefficient, it is necessary to know the flow velocity of the heat transfer fluid. In this context, methods to calculate

Znova je bilo ugotovljeno dobro ujemanje med obema metodama. Predloženo je bilo, kako se lahko oba značilna parametra pretvori v tehnične specifikacije.

Končno je bil opisan izračun prenosa topote za celotno kokilo za tlačno litje. Ta simulacija prikazuje učinkovitost optimizacije. Lahko se vidi, da obstaja določena možnost optimiranja klasičnih hladilnih sistemov. Vendar uporaba kokilnih vložkov, razdeljenih na segmente, da bi se prišlo do usklajenih hladilnih kanalov, celo presega zmožnost klasičnih hladilnih sistemov zaradi manj omejitev glede na površino za menjavo topote in razdaljo do površine. Zato je vredno nadaljevati z razvijanjem usklajenih hladilnih kanalov z delitvijo kokile za tlačno litje na segmente.

Zaradi izboljšav CFD-modelov, ki so v teku, se zdi, da je možno izvesti izboljšave učinkovitosti sistemov za reševanje in delovanja računalniških enot ter uporabe CFD-analize ter je smiselna izboljšava procesov konstruiranja kokil za tlačno litje. Trenutno smo ugotovili omejitve pri celotnem procesu modeliranja, ker je še vedno zelo zamuden.

Tehnične specifikacije, opisane v tem prispevku, bodo skrajšale ta postopek konstruiranja. Za veliko število kokil za tlačno litje je lahko ta metoda smiselna strategija. Vendar so hladilni kanali v obstoječih kokilah za tlačno litje često veliko preveč kompleksni, da bi prišli do rezultatov samo s temi tehničnimi specifikacijami. Enako velja za usklajene hladilne kanale, do katerih se pride s strategijami delitve na segmente ali z dodatno izdelanimi kanali. Zato je zaželeno, da se pri procesu konstruiranja uporabi celotna izvedba in se s tem pride do natančnega poznavanja porazdelitve temperature.

the friction factor of cooling elements with the commercial CFD software ANSYS CFX were described. The calculated results were compared to the results from experimental investigations and a good accordance has been found. Furthermore, the finite element code was used to model the heat transfer between the heat transfer fluid and the die-casting die. Reasonable accordance between both methods was found again. It was suggested how both characteristic parameter can be transformed into engineering specifications.

Finally, the calculation of the heat transfer within an entire die-casting die was depicted. This simulation illustrated the efficiency of the optimization. It could be shown that there is a considerable potential to optimize conventional cooling systems. However, the application of segmented die inserts in order to achieve conformal cooling channels even excels the capacity of conventional cooling systems due to fewer restrictions in regard to the heat exchanging surface and surface distance. Hence, it is worth-while to establish and to advance the development of conformal cooling channels by the segmentation of die-casting dies.

Due to an ongoing enhancement of the CFD models, improvements in the efficiency of the solvers and in the performance of computing units, the utilization of the CFD analysis appears to be feasible and reasonable to enhance the design process of die-casting dies. At this time, the restrictions are founded on the whole modeling process which still can be regarded as very time-consuming.

The engineering specifications described in this article shall serve to shorten this design process. For a large number of die-casting dies, this method is might be a sensible strategy. However, cooling channels of existing die-casting dies are often far too complex to derive results

## 6 Zahvala

Avtorji se želijo zahvaliti Nemški zvezi industrijskih raziskovalnih organizacij za finančno podporo temu raziskovalnemu projektu (projekt št. 17.210N).

only from these engineering specifications. The same applies to conformal cooling channels that originate from segmentation strategies or from additive manufacturing. Thus, the complete implementation into the design process is desirable in order to gain a precise knowledge about the temperature distribution.

## 6 Acknowledgements

The authors would like to express their honest gratitude to the German Federation of Industrial Research Associations for funding this research project (project no. 17.210N).

## 7 Viri / Literature

- [ANS10a] NM: ANSYS CFX-Solver Theory Guide, Release 13. Non-conventional literature of ANSYS Inc. Canonsburg, 2010
- [ANS10b] NM: ANSYS CFX-Solver Modeling Guide, Release 13. Non-conventional literature of ANSYS Inc. Canonsburg, 2010
- [BAE12] Baehr, H. D.; Stephan, K.: Heat and Mass Transfer. Springer-Verlag, Heidelberg, 2011.
- [EGG11] Eggenspieler, G.: Turbulence Modeling. Presentation, 2011 ANSYS Conference & ESSS Users Meeting, Brazil, 2011
- [LAU09] Laurien, E.; Oertel, H.: Numerische Strömungsmechanik. Vieweg+Teubner Verlag, Wiesbaden, 2009
- [LI05] Li, S.; Ueda, A.; Sanakanishi, S.; Mine, K.; Anzai, K.: Evaluation and application of thermal-oil/die heat transfer coefficients in thermal simulation. CastExpo Transactions, NADCA Congress, 2005
- [LIN03] Lin, J. C.: The optimal design of a cooling system for a die-casting die with a free form surface. The International Journal of Advanced Manufacturing Technology, Volume 21, PP. 612-619, 2003
- [MAR06] NM: Product Information MARLOTHERM® LH Heat Transfer Fluid <http://www.zhilichem.com/hg/MTHERMLH.pdf> Sasol North America Inc., 2006
- [MEN99] Menges, G.; Mohren, P.: Anleitung zum Bau von Spritzgießwerkzeugen. Carl Hanser Verlag, München, 1999
- [MUE12] Müller, R.: Innovation im Bereich der Sprühtechnik. Presentation, BDG Fachausschuss Druckguss, Germany, 2012
- [NOG10] Nogowizin, B.: Theorie und Praxis des Druckgusses. Schiele & Schön Verlag, Berlin, 2010
- [SIG12] Sigloch, H.: Technische Fluidmechanik. Springer-Verlag, Heidelberg, 2012
- [VDI06] NM: VDI Wärmeatlas. Springer Verlag, Heidelberg, 2006

## Preiskava trdnostnih lastnosti ulitkov za avtomobilsko industrijo, izdelanih iz livenih Al-Si zlitin

### The examination of the strength properties on the vehicle industry castings produced from Al-Si foundry alloys

#### Izvleček

Na dinamično razvijajočem se področju izdelave ulitkov za avtomobilsko industrijo se srečujemo z vse strožjimi zahtevami glede obratovalnih razmer. Danes se v liversko proizvodnji vse več uporablja zlitine iz sekundarnih surovin, vendar vpliv nečistot na te zlitine ni dobro znan. Pomembno je vedeti, da je količina nečistot v zlitinah Al-Si povezana s kakovostjo osnovnega materiala. Za modifikacijo silicijeve faz v teh zlitinah se uporablja predvsem dva elementa, nekatere liverske uporabljajo za to stroncij, druge antimon. Po reciklirjanju odpadkov se oba elementa nahaja v talini skupaj in lahko pride do nastanka intermetalnih spojin. Cilj naše raziskave je bil ugotoviti skupni vpliv antimona in stroncija v aluminij-silicijevih zlitinah in grafično prikazati nastanek intermetalnih spojin v talini ter njihov vpliv na kakovost končnih izdelkov. Članek prikazuje vpliv antimona in stroncija na mehanske lastnosti ulitkov pri različnih debelinah sten.

**Ključne besede:** aluminijeve zlitine, modifikacija silicija, debeline sten, mehanske lastnosti

#### Abstract

In the dynamically developing casting production area the vehicle casting productions must be met for more conditions in the interest of the performance of the increasingly stringent requirements. Nowadays secondary alloys are most frequently used in casting production, but the effects of the impurity elements on secondary alloys are not well known. It's very important to know that the quantity of impurity elements in the Al-Si alloys are related with base material quality. Mainly two elements are used to modify the eutectic silicon phase in these alloys, some foundries apply strontium, others modify with antimony. After the scrap recycling these elements are together in the melt, and the strontium and antimony together may be a cause for forming intermetallic compounds. The aims of the our research work were the examination of joint effects of antimony and strontium in aluminum-silicon alloys and to chart intermetallic compounds forming in melt and influencing quality in the final product. This paper presents the influence of antimony and strontium on mechanical properties in case of different wall thicknesses.

**Keywords:** aluminium alloys, silicon modification, wall-thicknesses, mechanical properties

## 1 Uvod

Izraz modifikacija opisuje postopek, s katerim se dodaja v talino aluminija cepivo v obliki predzlitin, da se spodbudi nastajanje nitastega evtektičnega silicija med strjevanjem [1]. Modifikacija silicija je splošen postopek, ki se uporablja pri aluminij-silicijevih livarskih zlitinah predvsem za izboljšanje mehanskih lastnosti, v največji meri raztezka, s spodbujanjem udobrjenja prvotno krhke silicijeve faze. Znano je, da dodatki stroncija v sledovih povektskem aluminij-silicijevim zlitinam povzročijo pretvorbo morfologije evtektičnega silicija iz grobe ploščičaste oblike v zelo drobno nitasto obliko [2]. Nečistote lahko poslabšajo učinek modifikacije in s tem mehanske lastnosti.

Pri našem delu smo ulili vrsto vzorcev z različnimi koncentracijami antimona in stroncija. Območji koncentracij sta bili 0 – 300 ppm stroncija in 0 – 340 ppm antimona. Izdelali in preskusili smo modelne ulitke različnih debelin sten (6 mm, 8 mm, 12 mm, 25 mm) ter iz njih izdelali natezne preizkušance.

## 2 Eksperimentalni del

### 2.1 Konstruiranje kokile za ulivanje

Da bi lahko primerjali vzorce z industrijskimi ulitki, smo konstruirali geometrijo ulitkov z različnimi debelinami sten. Kot se to vidi na shematičnem prikazu kokile (slika 1), so imeli vzorci 4 različne debeline stene, iz njih pa so bili narejeni natezni preizkušanci (premera 6 mm). Geometrijo ulitkov smo konstruirali z računalniškim programom Solid Edge. Nato smo z različnimi geometrijami ulitkov in napajalniki pripravili simulacije litja in iz dobljenih rezultatov izbrali najustreznejšo geometrijo. Računalniška oprema za

## 1 Introduction

The term »modification« describes the method in which inoculants in the form of master alloys are added to an aluminum melt in order to promote the formation of a fine and fibrous eutectic silicon structure during the solidification process [1]. Eutectic modification is a common process performed in aluminium–silicon based foundry alloys primarily to improve mechanical properties, particularly tensile elongation, by promoting a structural refinement of the inherently brittle eutectic silicon phase. It is well known that trace additions of strontium to hypoeutectic aluminium–silicon alloys result in a transformation of the eutectic silicon morphology from a coarse plate-like structure to a well-refined fibrous structure [2]. The impurities can deteriorate modification effect, thereby mechanical properties.

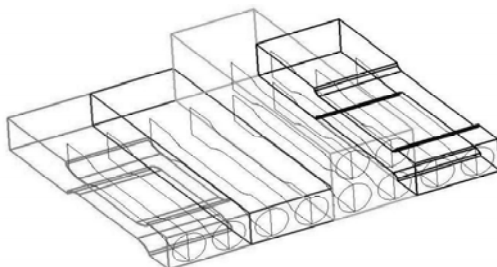
During our work we casted series from melt with different contents of antimony and strontium. The ranges of contents were between 0-300 ppm strontium and 0-340 ppm antimony. We constructed and tested a casting geometry with variable wall thicknesses (6mm, 8mm, 12mm, 25mm), and by using it we poured castings and tensile rods were processed from it.

## 2 Experimental conditions

### 2.1 Designing the casting die

In order to comparability with industrial castings we designed a casting geometry with different wall thicknesses. It can be seen on the schematic casting die with 4 different wall-thicknesses (Fig. 1.) and inside it there are the tensile rods (6 mm diameter). We designed the casting geometry by using

simulacije je bila NovaFlow in Solid. Po simulacijah smo izdelali kokilo za litje.



**Slika 1.** Shematični prikaz ulitka za natezne preizkušnace.

**Figure 1.** Schematics of the casting with tensile rods

## 2.2 Parametri in faze preskušanja

Za poskusno ulivanje smo uporabili ingote kupljene zlitine kakovosti AlSi9Cu3 ter predzlitino AISr10 v obliki žice in bloke predzlitine AISb10.

Stalili smo 100 kg blokov zlitine AlSi9Cu3 ter ulili štiri poskusne serije. Predzlitine smo dodajali v vsaki poskusni serijski (25 kg) v štirih korakih. Razpredelnica 2 prikazuje koncentracijo stroncija in antimona v vsaki od 4 serij. Antimon se je dodajal talini na začetku procesa litja in v vsaki od poskusnih serij se je koncentracija stroncija povečevala od 0 do 300 ppm. Po vsakem dodatku modifikatorja (Sb, Sr) smo talino pustili stati pri konstantni temperaturi 15 minut.

Razpredelnica 3 prikazuje parametre poskusov za vsako serijo.

Solid Edge software. We made casting simulations with some different geometries of casting and feeders, and by right of results we selected the best one. The simulation software was NovaFlow and Solid. After the simulation processes the casting die was produced.

## 2.2 Parameters and steps of the experiment

During the experimental casting we used manufacturer quality AlSi9Cu3 alloy ingots, the chemical composition is given in Table 1.. We used AISr10 (Al-10%Sr, wire) and AISb10 (Al-10%Sb, ingots) master alloys.

A total amount of 100 kg of the AlSi9Cu3 alloy ingots was melted and casted in 4 experimental series, and we alloyed every experimental series (4x25 kg) in 4 steps. The strontium and antimony alloying matrix of the 4 experimental series can be seen in Table 2. The antimony was added to melt at the beginning of the 4 casting processes, and in every experimental series the strontium content increased from 0 to 300 ppm. After every modifier element (Sb, Sr) addition the melt was holding at unvarying temperature for 15 minutes.

In Table 3. the experimental parameters can be seen which are unvarying at every casting series.

During the experiment we have used thermal analysis, dichte-index and spectral analysis. In order to monitoring the heat equilibrium the temperature of the casting

**Razpredelnica 1.** Kemična sestava aluminijevih zlitih AlSi9Cu3, uporabljenih za poskuse

**Table 1.** Chemical composition of the AlSi9Cu3 aluminum alloys used in experiments

Elementi / Elements	Si	Cu	Sr	Sb	Fe	Cr	Mn	Ca	P	Pb	Sn	Mg	Ni	Ti
mas. %	9,32	3,00	0,0005	0,0041	0,51	0,02	0,37	0,0014	0,0017	0,047	0,014	0,31	0,037	0,097

**Razpredelnica 2.** Koncentracija stroncija in antimona v poskusnih zlitinah

**Table 2.** The strontium and antimony alloying matrix of the experiment

serija / casting series	Stroncij / Strontium (ppm)	Antimony / Antimony (ppm)		
1.	5 (osnovna zlinita) / (base alloy)	40	140	240
2.	100		340	
3.	200			
4.	300			

Pri poskusu smo uporabili termično analizo, ugotavljali indeks gostote ter napravili spektralno analizo. Za nadzorovanje toplotnega ravnotežja smo s termodvojico zvezno merili temperaturo kokile za litje.

### 3 Rezultati analize mehanskih lastnosti

Za ugotavljanje mehanskih lastnosti smo izdelali iz ulitih vzorcev natezne preizkušance, kot kaže slika 2. Mehanske lastnosti smo ugotavljali z elektromehanskim nateznim strojem Instron 5982 pri natezni hitrosti 0,004 mm/mm/s.

Vpliv Sr-Sb na rezultate nateznih preskusov je verjetno manjši kot na druge parametre litja, zato se tega vpliva pri naših razmerah litja ne more ugotoviti. Vidimo, da smo najboljše mehanske rezultate dosegli pri debelini stene 8 mm. To se da razložiti z dejstvom, da je bilo napajanje najbolj učinkovito ravno pri debelini stene 8 mm. Pri debelinah stene 6 mm in 8 mm učinka Sr-Sb ni bilo opaziti zaradi hitrega strjevanja pri veliki strjevalni hitrosti. Pri debelini stene 25 mm pa poslabšanje mehanskih lastnosti verjetno povzroči vpliv Sr-Sb.

**Razpredelnica 3.** Parametri poskusov

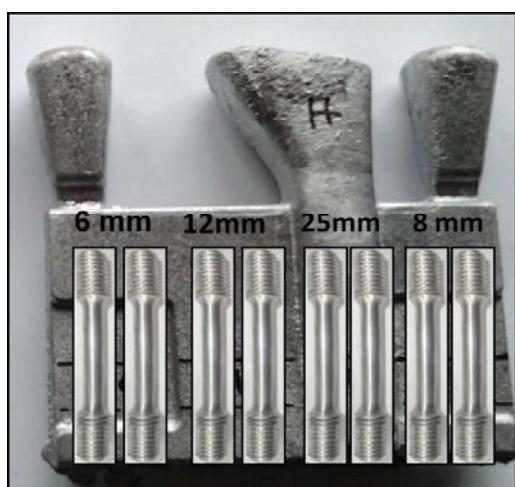
**Table 3.** The experimental parameters

Temperatura taljenja in legiranja / Melting and alloying temperature	(775±5)°C
Temperatura litja / Casting temperature	(765±5)°C
Predgrevanje kokile za litje / Preheating temperature of the casting die	400 °C
Čas zadrževanja taline po legiranju / Holding time after the alloying	15 min

die was measured by thermocouple continually.

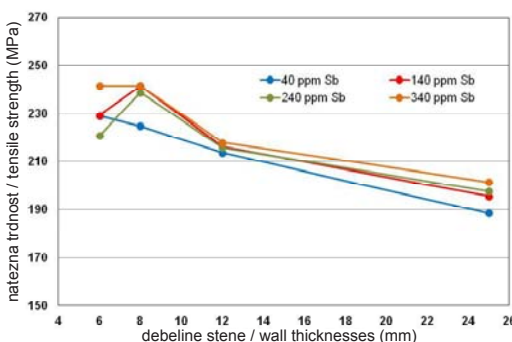
### 3 Results of the Mechanical Properties Analysing

To determine the mechanical properties tensile rods were processed from the places you can see in Fig.2. For analysing we used Instron 5982 electromechanical tensile test machine and the tensile speed was 0.004 mm/mm/s.



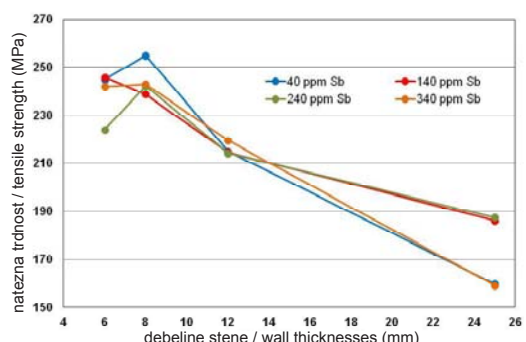
**Slika 2.** Ulitek in natezni preskušanci

**Figure 2.** Casting with tensile rods



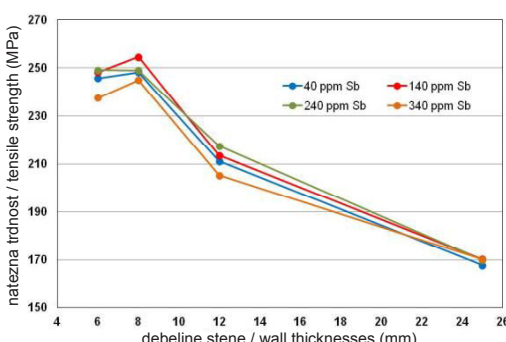
**Slika 3.** Povprečne natezne trdnosti v odvisnosti od debelin stene pri dodatku 5 ppm Sr

**Figure 3.** Average tensile strength values in function of wall thickness in case of 5 ppm Sr



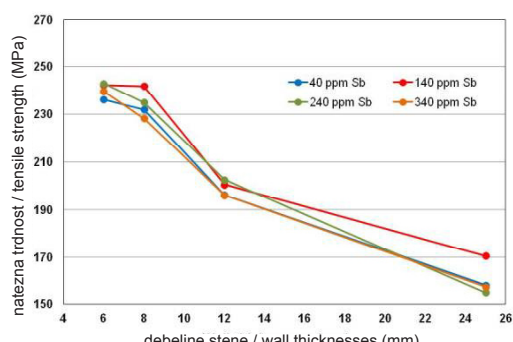
**Slika 4.** Povprečne natezne trdnosti v odvisnosti od debelin stene pri dodatku 100 ppm Sr

**Figure 4.** Average tensile strength values in function of wall thickness in case of 100 ppm Sr



**Slika 5.** Povprečne natezne trdnosti v odvisnosti od debelin stene pri dodatku 200 ppm Sr

**Figure 5.** Average tensile strength values in function of wall thickness in case of 200 ppm Sr



**Slika 6.** Povprečne natezne trdnosti v odvisnosti od debelin stene pri dodatku 300 ppm Sr

**Figure 6.** Average tensile strength values in function of wall thickness in case of 300 ppm Sr

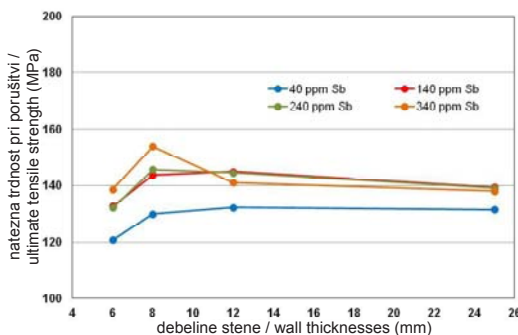
### 3.1 Rezultati meritev natezne trdnosti

Slike 3 do 6 kažejo rezultate meritev natezne trdnosti v odvisnosti od debeline stene pri koncentracijah stroncija 5 ppm, 100 ppm, 200 ppm in 300 ppm.

### 3.2 Največje natezne trdnosti

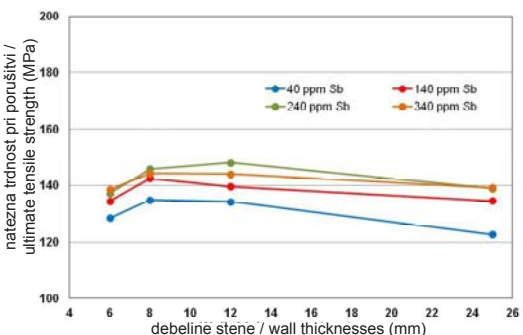
Slike 7 do 10 kažejo natezne trdnosti pri porušitvi v odvisnosti od debelin stene pri

The effect of Sr-Sb on the results of the tensile tests is probably smaller than that of the other casting parameters therefore their effect cannot be examined under present casting conditions. It can be seen that the best mechanical results were observed in castings with 8 mm wall thickness. This can be explained by the fact that the feeding of the casting is the most sufficient at the 8 mm wall-thickness. In the case of 6 mm and 8 mm wall-thicknesses the effect of Sr-Sb cannot be observed due to the rapid



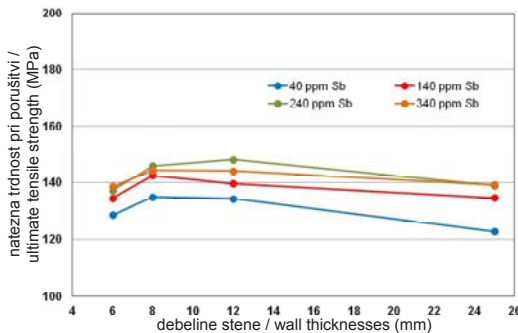
**Slika 7.** Povprečne natezne trdnosti pri porušitvi v odvisnosti od debelin stene pri dodatku 5 ppm Sr

**Figure 7.** Average tensile strength values in function of wall thickness in case of 200 ppm Sr



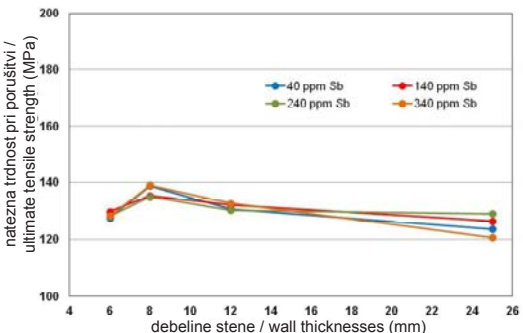
**Slika 8.** Povprečne natezne trdnosti pri porušitvi v odvisnosti od debelin stene pri dodatku 100 ppm Sr

**Figure 8.** Average tensile strength values in function of wall thickness in case of 300 ppm Sr



**Slika 9.** Povprečne natezne trdnosti pri porušitvi v odvisnosti od debelin stene pri dodatku 200 ppm Sr

**Figure 9.** Average tensile strength values in function of wall thickness in case of 200 ppm Sr



**Slika 10.** Povprečne natezne trdnosti pri porušitvi v odvisnosti od debelin stene pri dodatku 300 ppm Sr

**Figure 10.** Average tensile strength values in function of wall thickness in case of 300 ppm Sr

dodatkih 5 ppm, 100 ppm, 200 ppm in 300 ppm stroncija.

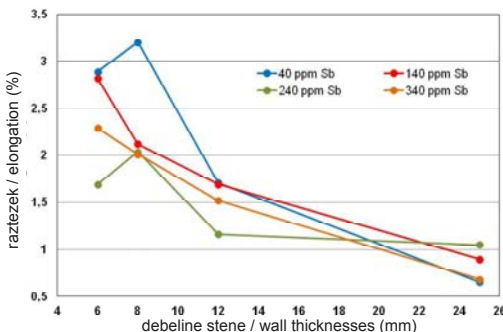
### 3.3 Rezultati meritev raztezka

Slike 11 do 14 kažejo rezultate meritev raztezkov v odvisnosti od debelin stene za dodatke 5 ppm, 100 ppm, 200 ppm in 300 ppm stroncija.

solidification caused by the high cooling rate. However, in the case of 25 mm wall-thickness the decrease of the mechanical properties is probably caused by the effect of Sr-Sb.

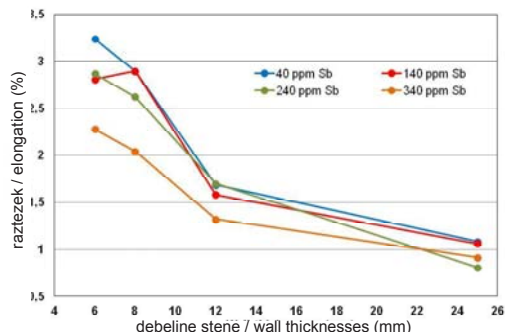
#### 3.1 Tensile Strength Results

In Fig.3 – Fig.6. it can be seen tensile strength results in function of wall-



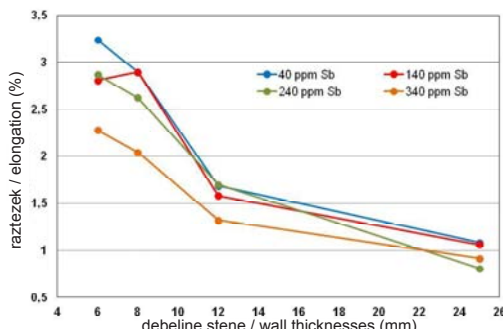
**Slika 11.** Raztezki v odvisnosti od debelin stene pri dodatu 5 ppm Sr

**Figure 11.** Average tensile strength values in function of wall thickness in case of 200 ppm Sr



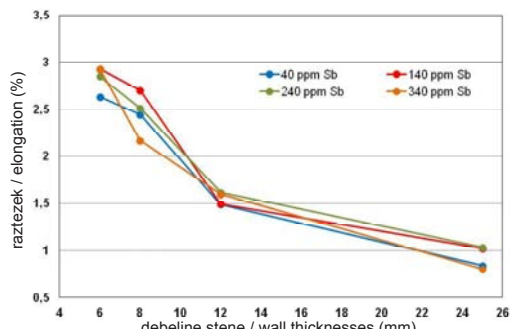
**Slika 12.** Raztezki v odvisnosti od debelin stene pri dodatu 100 ppm Sr

**Figure 12.** Average tensile strength values in function of wall thickness in case of 300 ppm Sr



**Slika 13.** Raztezki v odvisnosti od debelin stene pri dodatu 200 ppm Sr

**Figure 13.** Average elongation values in function of wall thickness in case of 200 ppm Sr



**Slika 14.** Raztezki v odvisnosti od debelin stene pri dodatu 300 ppm Sr

**Figure 14.** Average elongation values in function of wall thickness in case of 300 ppm Sr

## 4 Sklepi

V tej raziskavi so bili vzorci uliti iz aluminij-silicijeve zlitine z različnimi dodatki stroncija in antimona. Navezni preizkušnaci so bili izdelani iz ulitkov. Preiskan je bil vpliv antimona in stroncija na mehanske lastnosti v odvisnosti od debelin stene.

Da bi ugotavljali intermetalne spojine Sr-Sb, bomo prelomnine teh preizkušnancev preiskaliv prihodnosti. Vnašem dolgotrajnjem načrtu raziskav želimo preiskati mehanizem

thicknesses in case of 5 ppm, 100 ppm, 200ppm and 300ppm strontium.

### 3.2 Ultimate Tensile Strength Results

In Fig. 7 – Fig.10. it can be seen ultimate tensile strength results in function of wall thickness in case of 5 ppm, 100 ppm, 200ppm and 300ppm strontium.

### 3.3 Elongation results

In Fig.11 – Fig.14. it can be seen elongation results in function of wall thickness in case

vpliva elementov modifikatorja ter analizirati njihove medsebojne vplive. Najprej želimo spoznati osnovne procese zaradi tehnološke optimizacije in s prilagoditvijo parametrov industrijskim procesom zagotoviti, da se lahko s poskusi modelira težave in učinke, ki se pojavljajo med dejansko proizvodnjo.

of 5 ppm, 100 ppm, 200ppm and 300ppm strontium.

#### 4 Conclusion

In this work, samples were cast from different alloys with varying Sr-Sb content. Tensile test specimens were processed from the castings and the influence of antimony and strontium on mechanical properties were examined as a function of different wall thickness. The examination of the fracture surfaces of these samples will be carried out in the future to identify the different Sr-Sb intermetallics. In our long-term research plan we would like to investigate the effect mechanism of modifier elements, and analyse its cross effects. Firstly we want to understand the basic processes in our research work, and to observe the technological options and by adapting the industry process parameters we would like to ensure that with experiments we can model the problems and affects which were occurred during the actual production.

#### 5 Viri / References

- [1] M.Djurđević, H.Jiang, J.Sokoliwski: On-line prediction of aluminium-silicon eutectic modification level using thermal analysis, Materials Characterization - Elsevier, 46(2001)31-38
- [2] A.K.Dahle, K.Nogita, S.D.McDonald, C.Dinnis, L.LucEutectic modification and microstructure development in Al-Si alloys, Materials Science and Engineering, A413-414(2005)243-248
- [3] N.Fatahalla, M.Hazif, M.Abdulkhalek: Effect of microstructure on the mechanical properties and fracture of commercial hypoeutectic Al-Si alloy modified with Na, Sb and Sr, Journal of Materials Science, 34(1999)3555-3564
- [4] S.A.Jenabali Jahromi, A.Dehghan, S.Malekjani: Effects of optimum amount of Sr and Sb modifiers on tensile, impact and fatigue properties of A356 aluminium alloy, Iranian Journal of Science&Technology, Transaction B, Vol. 28, No.B2, 2004

**AKTUALNO / ACTUAL**

# **EUROGUSS 2014**

## **Euroguss 2014 v Nuernbergu**

V času od 14. - 16. januarja letos je potekala specializirana sejemska prireditev EUROGUSS 2014 namenjena livarski tehnologiji tlačnega litja. Gre za prireditev, ki jo organizira vsako drugo leto, to pot že desetič, Nuernberški sejem. Vsi tisti, ki smo si prireditev ogledali pred dvemi leti, smo lahko videli vidni napredok in rast le-te letos, tako v številu obiskovalcev kot tudi razstavljalcev. Ob tem je zaznana občutna rast v smeri internacionalizacije te prireditve (30% izven Nemčije). Lahko bi rekli, da se je celotno evropsko tlačno livarstvo zgrnilo na to lokacijo, kar je dalo impozantno sliko o tem, kaj danes ta del livarstva premore oz. ponuja. Ta predstavitev je tudi pokazala, da je branža na poti vztrajne rasti in produktov visoke dodane vrednosti, leto 2014 pa obeta ugodna konjungturna gibanja.

Livarne, dobavitelji za livarsko industrijo in znanstvene organizacije so predstavile: ulitke, materiale, peči, stroje in orodja za litje, postopke za obdelavo ulitkov, postopke kontrole kvalitete kot tudi najnovejše razvojno znanstvene dosežke.

V ospredju je bila avtomobilska industrija, ki porabi ¾ evropskih livaških izdelkov, kot tudi področja strojogradnje in opreme, elektro in elektronske industrije ter inovativne industrijske panoge s področja energije in medicinske tehnike, ki so tudi dokaj veliki odjemalci livaških izdelkov.

Sejem EUROGUSS postaja tudi zelo zanimiv in razpoznaven za slovensko livaško industrijo. Na letošnjem sejmu so sodelovali: LTH Castings d.o.o., DIFAd.o.o., Kovinoplastika Lož d.d., Lama Avtomatizacija d.o.o, Orodjarstvo Gorjak d.o.o.

*Poročala: mag. Mirjam Jan-Blažič*



## AKTUALNO / ACTUAL



## 71. WFC- svetovni livarski kongres

V organizaciji Španije, kot članice WFO- Svetovne livarske organizacije oziroma Tabira Foundry inštituta in IK4-Azterlan, je v času od 19.-21.05.2014 potekal 71. WFC- Svetovni livarci kongres v Bilbao-u.

Predsednik WFO Vinod Kapur je v pozdravnem govoru na otvoritvi kongresa dejal: "Zdaj je čas, da se odzovemo v smislu iskanja novih izdelkov in procesov, ob upoštevanju trajnosti in moralne obveznosti, da smo okoljsko zavedni." Kongres je potekal pod motom "Napredno trajnostno livarstvo". Več kot 1000 udeležencev je v 3 dneh lahko poslušalo zanimiva strokovna predavanja in tudi sodelovalo na seminarju mladih študentov, programu mladih raziskovalcev, forumu livarskih kupcev, na mednarodni livarski razstavi kot tudi na obiskih v livenah.

Vsa predavanja, ki so bila predstavljena na kongresu, smo zgoščenki, katera je na razpolago za vse livenje - članice Društva livenje Slovenije. V primeru, da obstaja interes tudi pri drugih članicah Društva- dobaviteljih livarske industrije, nam sporočite naročilo zgoščenke na email: drustvo.livarjev@siol.net.

Kongres vsako drugo leto organizira ena od članic WFO. Kongres omogoča seznanjanje s aktualnimi tehničnimi in tehnološkimi dosežki na področju livarstva, vsem udeležence pa predstavlja priložnost za izmenjavo izkušenj.

Na kongresu so najboljše ocenjena predavanja prejela posebna priznanja:

- zlato priznanje: Dana Cooper, Fairmount Minerals Ltd, USA: '*Sustainability is the Key Driver of Innovation*'
- srebrno priznanje: Jaimie Prat, Ask Chemicals, Spain: '*Net/Gross Yield Optimisation of High Value Added Steel Castings*'
- bronasto priznanje: U Petzschmann IfG, Germany: '*Active Cooling of Resin Bonded Moulds to Reduce the Cooling Time of Heavy Section Castings Without Loss of Quality*'



G. Vinod Kapur, predsednik WFO

*mag. Mirjam Jan Blažič*

**IN MEMORIAM**

Jakob Mostar ob izvedeni formi

**In memoriam: Jakob Mostar**

Po daljši bolezni nas je nepričakovano in veliko prezgodaj zapustil prijatelj, zvesti stanovski brat, livar in metalurg, JAKOB MOSTAR, rojen 29.4.1975 v Ljubljani.

Jakob prihaja iz livarske družine Mostar, ki slovi po več kot 100 letni tradiciji livarstva. Osnovno šolo in srednjo strojno šolo je obiskoval v Ljubljani, kjer je že zanetil iskro ljubezni do livarstva. Diplomiral je leta 2001 na Univerzi v Ljubljani, Naravoslovnotehniški fakulteti, Odedelku za materiale in metalurgijo, Katedri za livarstvo, pod mentorstvom prof. dr. Milana Trbižana. Tema diplomskega dela je bila Merjenje aktivnosti kisika in termična analiza taline za indefinitne valje, ki jo je končal z odliko.

Ko sem na dopustu prejel klic, da je dragi in spoštovani Jakob preminil, me je globoko potrlo in prizadelo. Zavrtelo se mi je vse najino iskreno in plodno sodelovanje. Delila sva ljubezen do livarstva in metalurgije, pa tudi ko sva se bolje spoznala, ugotovila, da imava zelo podobne poglede na življenje in Slovenstvo. Lahko rečem, da je Jakob bil in je v naših srcih izjemnen Človek v pristnem pomenu te besede, saj je nudil pomoč in podporo mnogim, kot se spominjam še iz časa študija. Izstopal je kot najboljši študent generacije, inovator in delu predan človek.

Jakobova livarna, ki jo je z veliko predanostjo in ljubeznijo do metalurgije, postavil kot naslednik družinske tradicije, nam je dala veliko bronastih in aluminijastih izdelkov, zlasti je bil ponosen na nove oblike zvonov, ki so akustično in estetsko izjemno dovršeni. Tudi ulivanje umetnih, plaket in reliefov je bil zanj poseben izziv, ki se mu je rad posvečal, saj je s širjenjem svoje livarne želel uvesti tehniko ulivanja z iztaljivimi modeli (precizijsko litje). Sredi velikega zagona, ko je že prenovil prostore, zgradil nagibno talilno peč in z velikimi koraki stopal skozi življenje, nas je presenetil s svojim odhodom.

V svojem življenju je vzorno skrbel za starše, predano nadaljeval s podjetjem Livarstvo Mostar, se proslavil z zahtevnimi ulitki, bil športnik in predvsem kolegialen, inovativen ter delaven metalurg. Kar je mogoče še najpomembnejše – njegov blagi temperament in živ duh, s katerim si je odkrival nova obzorja in nas razveseljeval v človeškem in strokovnem smislu, sta ga zapisala v naša srca in zelo ga bomo pogrešali.

Težko razumemo njegov prehod h gospodarju življenja, saj je bil Jakob še poln načrtov in idej, smo pa prepričani, da je našel svoj mir in je skupaj s predniki. Tukaj nam ostajajo spomini nanj in njegova dela, ki krasijo Slovenijo in svet: Tvoji zvonovi, plakete, skulpture ter tehnični ulitki iz bakrovih in aluminijevih zlitin. Jakob, Srečno in nasvidenje nad zvezdami!

*prof. dr. Primož Mrvar in doc. Jurij Smole, ak. kipar*

**AKTUALNO / ACTUAL****DRUŠTVO LIVARJEV SLOVENIJE****SLOVENIAN FOUNDRYMEN SOCIETY****vas vladno vabi na / invites you to****55. MEDNARODNO LIVARSKO POSVETOVANJE****55<sup>th</sup> INTERNATIONAL FOUNDRY CONFERENCE****PORTOROŽ 2015****s spremljajočo razstavo / with accompanying exhibition  
16.-18. september 2015**

Informacije/Contact: Društvo livarjev Slovenije,  
Lepi pot 6, p.p. 424, 1001 Ljubljana, T: +386 1 2522 488, F: +386 1 4269 934  
[drustvo.livarjev@siol.net](mailto:drustvo.livarjev@siol.net), [www.drustvo-livarjev.si](http://www.drustvo-livarjev.si)